Chapter 8

Summary

Presents summary interpretations of topics that cover multiple time periods in the recorded history of Kīlauea, including long-term magma supply, south flank anticipation of eruptions and intrusions, history of south flank spreading, and the relation between the plumbing systems of Kīlauea and Mauna Loa Volcanoes.

Continuous GPS station HOLE, located on Holei Pali on the south flank of Kilauea Volcano. The GPS antenna is the white disk on the monument at the far right, while the antenna on the left side of the image transmits data back to the Hawaiian Volcano Observatory. The station is powered by solar panels (far left) that charge a bank of batteries, which reside, with the GPS receiver, in the hardened instrument box at the center of the photo. Photograph by M. Poland.

Our 200-year history of Kīlauea emphasizes the interpretation of magma transport and storage below the volcano surface in order to connect the long sequence of eruptive and intrusive activity as coherently as possible. For our interpretation we use the continuous record provided first by earthquakes and eruption chronology and later, following the founding of the Hawaiian Volcano Observatory, by tilting of the ground measured daily at Kīlauea's summit. We seek a long-term view of Kīlauea within which individual events and observations can be placed. Details of individual eruptions are provided by references cited in the text; our aim is to understand how each event in Kīlauea's history is affected by prior events and influences future events.

Magma Transport from Melting Source to Storage

Geometry of Kīlauea's Magma Plumbing

Magma destined for eruption at Kīlauea is generated by partial melting at depths of 80–100 km within a source region in the mantle designated as the Hawaiian hot spot. Evidence from long-period earthquakes indicates that most of Kīlauea's magma travels from initial melting at 80–100 km depth within the source region through a vertical (100–35 km depth) to horizontal (30±5 km depth) to vertical (above ~25 km depth) conduit to reach Kīlauea's summit magma chamber (Wright and Klein, 2006). Vertical transport from the mantle is aseismic to about 60-km depth as magma coalesces in a ductile region near the base of the lithosphere. Between 60-km depth and the base of the Kīlauea edifice at ~11-km depth, only about 10 percent of the energy associated with magma transport is released as a combination of long-period and short-period earthquakes (Aki and Koyanagi, 1981). In this realm the coalescing magma must maintain a hot core within a cooler shell in order to allow upward movement, much as magma transport in pāhoehoe lava is facilitated by the formation of lava tubes.

A shallow-dipping decollement at depths of 10–12 km separates the Kīlauea edifice from the older ocean floor and sediment layer present at Kīlauea's inception (Delaney and others, 1990). Magma transport through the edifice is accompanied by a much higher seismic response. A storage chamber has been identified at depths of 2–6 km beneath Kīlauea's summit caldera through modern seismic and geodetic study. The chamber consists of a small liquid core (see below) surrounded by magma-permeated rock, cool enough to result in rapid solidification of small packets of magma such that the carapace can continue to fracture during epsisodes of inflation and deflation. All magma passes through this chamber before eruption or intrusion at Kīlauea's summit or rift zones. We presume that such a chamber has existed throughout the shield-building stage of Kīlauea's history (Clague, 1987; Clague and Dixon, 2000). At different times in Kīlauea's history this magma chamber at 2–6 km depth has been augmented by a smaller magma storage chamber at a depth of 1 km or less, also beneath Kīlauea Caldera (fig. 8.1).

Below Kīlauea's rift zones, from 5-km depth down to the decollement, modern studies have postulated magma-permeated rock that is able to transmit pressure to the adjacent solid south flank. All of our historical research supports the existence of such a "deep [rift] magma system" (Delaney and others, 1990). Some-upward moving magma from the hot spot may be diverted to the deep rift magma system before reaching the reservoir, particularly during periods in which the plumbing is being repaired, such as following the 1975 earthquake or the 1924 intrusion. Such magma contributes to the increased magma pressure before eruptions or intrusions but is not itself erupted or intruded at shallow levels. Magma destined for eruption at the summit or on the rift zones is fed either from the liquid core within the main summit reservoir or from the shallower reservoir at about 1-km depth, as illustrated in figure 8.1. Magma destined for intrusion beneath the rift zones is diverted during upward transport below the liquid core, but still within the summit reservoir (fig. 8.1).

Petrologic Contribution to Understanding Magma Storage and Transport

In chapter 4 (fig. 4.13) we presented our interpretation of how the magmas having the chemistry of the three Halemaʻumaʻu eruptions of 1952, 1961, and 1967–68 moved through the rift plumbing. We can now address related questions regarding volumes of the three magma batches, where they entered the rift plumbing, and how long they remained before they were no longer seen in rift eruptions. Volumes of the magma batches seen in both summit eruptions and hybrid east rift eruptions are shown in table 8.1. Volumes of additional magma transferred to the east rift zone between eruptions are also tabulated in table 8.1.

The summit reservoir and its ability to hold magma in different volumes, as shown by the complexity of different internal reservoir deformation centers, is key to the eruption of distinct magma batches. The expected deformation field above expanding magma bodies of differing geometry, such as sills, dikes, or intrusive plugs, has been modeled by Dieterich and Decker (1975). Many deformation cycles documented in Hawaiian Volcano Observatory monthly reports (unpublished) show (1) a migration

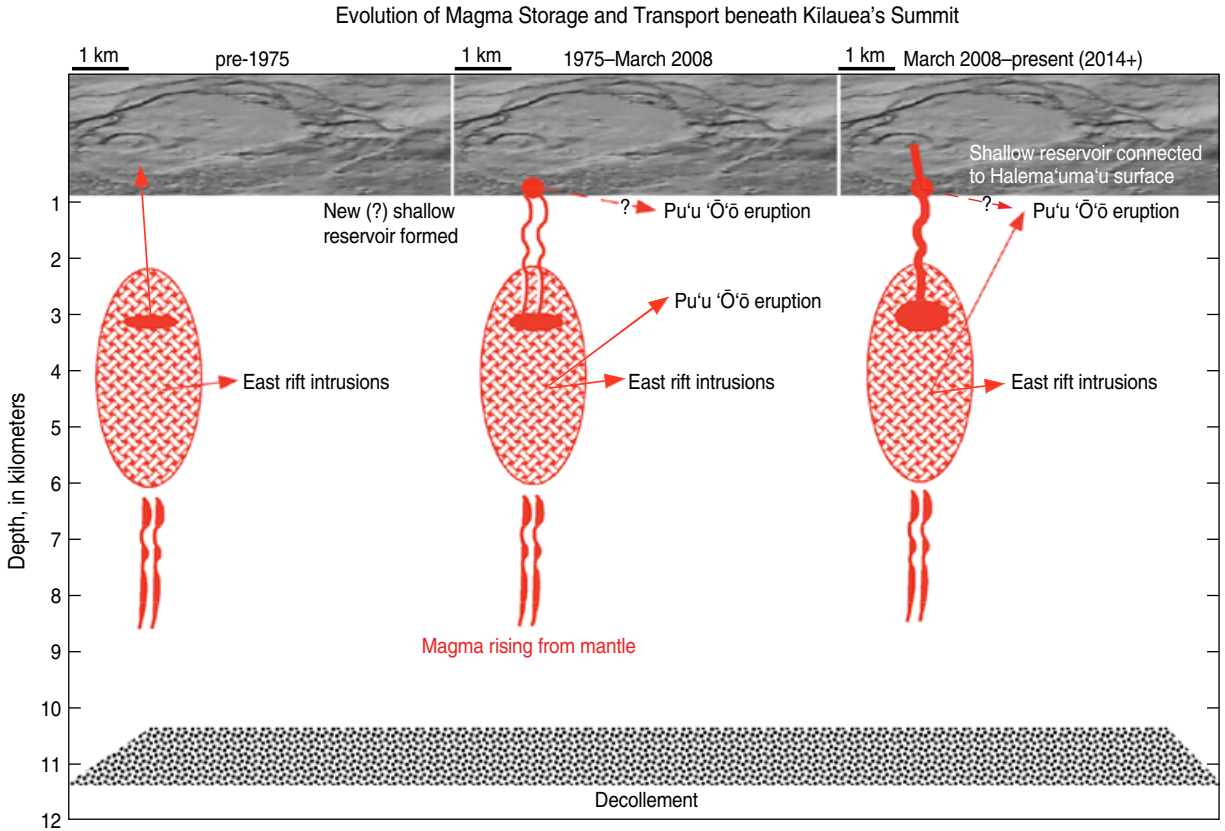

Figure 8.1. Diagram showing three stages in the evolution of Kīlauea's plumbing. Magma from the mantle (wavy red lines) feeds Kīlauea's primary reservoir at 2–6 km depth that supplies all magma for eruption and intrusion. A source depth of 3 km, calculated according to principles laid out by K. Mogi (1958), is shown, averaged from many leveling and tilt surveys. Summit eruptions are fed from a small liquid core within the larger reservoir (see fig. 8.2 and text discussion). Rift eruptions are diverted from the primary vertical conduit at some depth below the liquid core. See text for further discussion. Pre-1975 configuration: A single primary reservoir supplemented by a shallow (<1 km depth) reservoir (not shown) during summit lava lake activity. From 1975 to March 2008: Configuration after appearance of shallow magma reservoir northeast of Halema'uma'u at a depth of less than 1 km. Such a reservoir was also present during the 19th and early 20th century to feed Kīlauea's lava lakes. The interpretation that Pu'u 'Ō'ō is being fed from the reservoir at 1 km depth (Cervelli and Miklius, 2003) has been revised to favor a source within the traditional reservoir at 2-6 km depth (M. Poland, oral commun., 2012). March 2008 to present: Breakdown of the connections between the two reservoirs and the surface, leading to explosive eruption at Halema'uma'u and the existence of a sub-Halema'uma'u lava lake.

of inflation and deflation centers similar to that described by Fiske and Kinoshita (1969) and (2) a greater lateral extension of lines spanning the caldera than that predicted by the spherical Mogi source approximation, implying a larger vertical than horizontal extent of the expanding magma body. We adopt a summit plumbing model of concatenated vertical plugs, following the analysis of Dieterich and Decker (1975), that fits both the migrating centers of inflation and the observed summit ground-deformation patterns (fig. 8.2). The protrusions at the top of the chamber in the figure represent the tops of vertical plugs at the location of the most commonly occupied centers of deflation and inflation.

The volumes of the magma batches erupted at Kīlauea's summit in 1952, 1961, and 1967–68 range from 0.13 to 0.21 km^3 (table 8.1). We use an average area of 1 km^2, based on the extent of the preferred south caldera inflation-deflation centers, and a maximum storage volume of 0.09 km^3 derived from the volumes of magma erupted in Halema'uma'u. These assumptions yield a thickness of the active

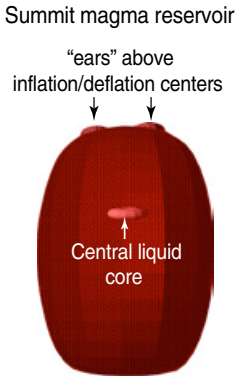

Figure 8.2. Diagram of Kīlauea's primary magma reservoir. The reservoir is outlined as a magma-permeated zone of concatenated vertical plugs surrounding a much smaller liquid core. The vertical plugs lie above the inflation/deflation centers defined in the buildup to the 1967–68 Halema'uma'u eruption (see fig. 4.2) and are manifested as "ears" sprouting from the reservoir top. The diagram is not to scale, but the larger reservoir is 1–2 km across and extends vertically as much as 4 km, and the liquid core is estimated at tens of meters in diameter.

Table 8.1. Volumes of magma batches entering Kīlauea plumbing.

[dates in m/d/yyyy format; V, volume; do, ditto (same as above)]

a. Magma erupted in homogeneous summit eruption or mixed in hybrid eruptions.

Name	Start date	End date	V (km^3)	Comment	Reference[1]
1952	6/27/1952	11/9/1952	0.0870	Halema‘uma‘u eruption	4
	3/20/1955	5/26/1965	0.0333	Later part of 1955 eruption; mixing percentage 41.9	9, 1
	1/26/1960	1/29/1960	0.0035	Early part of 1960 eruption; mixing percentage 35.7	9, 2
Total			0.1335		
1954	5/31/1954	6/3/1954	0.0050	Kīlauea Caldera eruption	8
	11/14/1959	11/21/1959	0.0042	1959 eruption episode 1: mixing percentage 45.5	5, 3
	11/22/1959	12/20/1959	0.0027	1959 eruption episodes 2–17: mixing percentage 13.2	5, 3
Total			0.0119		
1961	3/5/1955	3/6/1955	0.0418	Kalalua intrusion—calculated as parent for 1977 eruption	9,
	1/30/1960	2/4/1960	0.0086	Middle part of 1960 eruption; mixing percentage 58.2	5, 2
	2/24/1961	7/17/1961	0.0103	Halema‘uma‘u eruptions (3)	6
	9/22/1961	9/25/1961	0.0390	East rift eruption: assume 1961 and 1967 in equal volume	6, 15
	12/7/1962	12/9/1962	0.0049	12/1962 east rift eruption	14, 15
	8/21/1963	8/23/1963	0.0022	8/1963 east rift eruption	10, 15
	10/5/1963	10/6/1963	0.0155	10/1963 east rift eruption	11, 15
	3/5/1965	3/15/1965	0.0033	3/1965 east rift eruption	12, 15
	12/24/1965	12/25/1965	0.0036	12/1965 east rift eruption	13, 15
Total			0.1292		
1967–68	2/12/1960	2/18/1960	0.0043	Later part of 1960 eruption: mixing percentage 24.8	5, 2
	9/22/1961	9/25/1961	0.0390	East rift eruption: assume 1961 and 1967 equal volume	6, 15
	12/7/1962	12/9/1962	0.0064	12/1962 east rift eruption	14, 15
	8/21/1963	8/23/1963	0.0016	8/1963 east rift eruption	10, 15
	10/5/1963	10/6/1963	0.0250	10/1963 east rift eruption	11, 15
	3/5/1965	3/15/1965	0.0381	3/1965 east rift eruption	12, 15
	12/24/1965	12/25/1965	0.0177	12/1965 east rift eruption	13, 15
	11/5/1967	7/14/1968	0.0744	Halema‘uma‘u eruption	7
	8/22/1968	8/28/1968	0.0024	8/1968 east rift eruption	16, 18
	10/7/1968	10/22/1968	0.0234	10/1968 east rift eruption	16, 18
	2/22/1969	2/28/1969	0.0061	2/1969 east rift eruption	17, 18
Subtotal			0.2384		
Total			0.5130	Total amount of unfractionated magma identified[2]	

[1]Helz and Wright, 1992; 2. Wright and Helz, 1996; 3. Wright, 1973; 4. Macdonald, 1952; 5. Richter and others, 1970; 6. Richter and others, 1964; 7. Kinoshita and others, 1969; 8. Macdonald and Eaton, 1954; 9. Macdonald and Eaton, 1964; 10. Peck and Kinoshita, 1976; 11. Moore and Koyanagi, 1969; 12. Wright and others, 1968; 13. Fiske and Koyanagi, 1968; 14. Moore and Krivoy, 1964; 15. Wright and Fiske, 1971; 16. Jackson and others, 1975; 17. Swanson and others, 1976b; 18. Wright and others, 1975.

[2]Add 0.01 km3/year for rift dilation during spreading; lifetime of magma batches ~ 10 years.

b. Additional magma transfer to east rift zone: deflation volumes not associated with eruption.

Start date	End date	V (km^3)	Comment
9/15/1950	12/8/1950	0.0088	Assumed to be magma batch of 1952 chemistry
12/8/1950	12/16/1950	0.0507	do
Subtotal		0.0595	Minimum volume1952 magma intruded into the rift zone.
6/26/1952	10/2/1952	0.0323	Assumed to be magma batch of 1961 chemistry
3/10/1954	3/24/1954	0.0082	do
12/13/1954	1/17/1955	0.0114	do
2/19/1955	12/29/1955	0.1494	do
8/31/1959	11/14/1959	0.0011	do
Subtotal		0.2024	Volume of 1961 magma intruded into the east rift zone
11/15/1959	11/23/1959	0.0213	Assumed to be magma batch of 1967–68 chemistry[3]
12/23/1959	1/17/1960	0.0103	do
1/17/1960	10/21/1960	0.1405	do
9/21/1961	9/30/1961	0.0779	do
10/28/1961	11/4/1961	0.0046	do
12/6/1962	12/9/1962	0.0092	do
5/8/1963	5/12/1963	0.0157	do
6/28/1963	7/2/1963	0.0085	do
8/21/1963	8/22/1963	0.0036	do
10/4/1963	10/10/1963	0.0362	do
11/11/1964	12/1/1964	0.0022	do
3/5/1965	3/9/1965	0.0395	do
12/23/1965	12/29/1965	0.0213	do
10/1/1966	10/7/1966	0.0044	do
8/9/1967	8/18/1967	0.0038	do
Subtotal		0.399	Maximum additional volume of 1967-68 chemistry. May include some 1961 chemistry.
Total		0.6609	

[3]Latest time that magma can enter east rift zone for mixing with the latter part of the 1960 eruption.

storage region of about 115 m, which is sufficient to prevent cooling during the brief time in storage. Mogi models from levelling measurements suggest that this zone of stored high-temperature liquid lies about 3 km below Kīlauea's summit. The percentage of liquid magma within the whole of the seismically and geodetically imaged summit reservoir is quite small. Assumed spherical reservoirs of radii 1 and 2 km yield reservoir volumes of 4.19 and 33.51 km^3, respectively. The estimated percentage of magma to solid rock in storage ranges between 0.3 and 2.1 percent. We consider that magma for the 1952, 1961, and 1967–68 Halema'uma'u eruptions successively occupied a small liquid region like that shown in figure 8.2 and moved from there to eruption in Halema'uma'u as shown in figure 8.1. The fact that each of the three summit eruptions retained a different but uniform chemistry indicates that each magma batch had to be totally removed by eruption before the next magma entered[28].

During each magma batch's time in storage, a variable but high percentage of the magma was partitioned to the east rift zone. The fact that the magmas are seen as components of rift eruptions even before they are seen in Halema'uma'u indicates that they cannot move into the rift zone from the liquid core beneath the caldera, but must move into the rift zone from some greater depth before the liquid core is ready for a new batch of magma to enter from below, as depicted in figure 8.1. The depth at which transfer to the rift occurs can be determined by the CO_2 content of the magma erupted on the rift zone, which averages 0.05 weight percent (Gerlach and others, 2002). That level of CO_2 corresponds to an equilibrium pressure of ~ 1.1 kbar, corresponding to a depth of 4–5 km (Dixon and others, 1995). The transfer depth of 4–5 km places magma in a position to feed the main rift magma conduits at depths of 2–4 km.

Magma occupation of the primary summit reservoir changed in the years following the 1967–68 summit eruption. Beginning with the two 1968 rift eruptions, 10 new olivine-controlled magmas appeared during 1968–75. (Wright and Klein, 2010). Magmas erupted at Mauna Ulu during 1969–74 suggest a more complex hybridization in which olivine-controlled magmas could have been mixed with each other before eruption. The magma batches were smaller in volume than the 1952, 1961, and 1967–68 batches, and thus more than one batch could simultaneously occupy the liquid core depicted in figure 8.2.

The April 1982 summit eruption can be interpreted as a mixture of the two most voluminous magma compositions erupted at Mauna Ulu. Eruptions on the rift zone in 1979 and 1980 were complex mixtures of several olivine-controlled magmas, some of which had undergone limited fractionation. We attribute the greater frequency of chemical changes among magma batches and the resultant more complex mixing to documented increases in magma supply rate. The smaller volume of magma baches allows them to simutaneously occupy the storage area formerly occupied by a single magma batch, thus promoting mixing (see footnote above).

The eruption that began in 1983 has been accompanied by further dramatic increases in magma supply rate, and all vestiges of a sequence of distinct olivine-controlled magmas are gone. A more subtle and continuous variation has been ascribed variously to changes in the chemistry of the source mantle (Marske and others, 2008) or to mixing and flushing of previously existing olivine-controlled magmas by new magma derived from a mantle of constant source chemistry (Thornber, 2001).

Relation Between Eruption and Intrusion Expressed as Eruption Efficiency

Eruption efficiencies (compare Wright and Klein, 2008, their figure 6 and discussion) have been calculated as a ratio of the volume erupted (after correction for vesicularity) to the volume of magma transferred to feed a rift eruption as estimated from the Uwēkahuna tilt deflation magnitudes. Eruption efficiency is a measure of the state of the rift-zone magma plumbing, the confining stress, and the ability of the rift to allow magma to move to the surface. Eruption efficiency estimates magma partitioning between eruptions and intrusions, an alternative to the presentation of eruption/intrusion balances by Dvorak and Dzurisin (1993, figure 10). Eruption efficiencies are plotted in figure 8.3 for the period preceding the 1975 earthquake (fig. 8.3*A*) and during stage IA of the Pu'u 'Ō'ō-Kupaianaha eruption (fig. 8.3*B*). Eruption efficiency is low following a long interval without rift eruption, because magma must fill rift voids created during ongoing flank spreading, and it takes a larger magma pressure and volume to open new conduits to the surface. Eruption efficiency then increases as the rift plumbing becomes hot through repeated use and as conduit widths increase. Reversals to low eruption efficiency shown in figure 8.3*A* are associated with Koa'e activity, possibly because the Koa'e Fault Zone, upon being intruded with rift magma, wedges the east rift apart, forming voids to hold future intrusions without eruption. The Koa'e itself acts as a magma sink, rarely erupts, and so has near-zero eruption efficiency. Lower eruption efficiencies may also follow some suspected deep intrusions on the assumption that some of these intrusions are associated with rift dilation. Magma pressure generated during the suspected deep intrusions in

[28] If two magmas of similar density enter the liquid chamber, the earlier magma will be more degassed and thus more dense than the new arrival, thus promoting mixing of the two magmas.

August and November 1965 (table 4.1; fig. 4.12) may have been one cause of the Koa‘e crisis in December 1965. During Mauna Ulu stage IA from May to December 1969, a brief relative reduction in eruption efficiency followed suspected deep intrusions (fig. 8.3*A*).

Eruption efficiencies for the high-fountaining episodes beginning the Pu‘u ‘Ō‘ō-Kupaianaha eruption (fig. 8.3*B*) scatter widely, but the average is close to 1, as might be expected for a long eruption with little accompanying intrusion. There are significant uncertainties in both the estimates of deflation magnitude and episode volumes. The deflation azimuths from Uwēkahuna given in table 7.1 point to centers between Fiske-Kinoshita centers 1 and 2. Eruption efficiencies for azimuths that point to center 1 are close to 1 at an average depth to the Mogi source of 3.6 km (appendix A, table A1). More northerly azimuths at the same depth require a factor that reduces the eruption efficiency by only 1 percent. To achieve an average eruption efficiency of 1 only by adjusting the volume calculated from tilt magnitude requires depths greater by less than 0.5 km, well within the uncertaintiy in depth determination from Mogi models. Eruption volumes are also uncertain, particularly as flow thickness could only be measured at flow edges (Wolfe and others, 1988, p. 6 and following). Within these uncertainties we cannot reject the null hypothesis that the eruption efficiency during stage IA was 1, meaning that all magma supplied was erupted. This represents a marked departure from earlier periods and attests to the adjustment of the magma transport path to accommodate all magma as eruption rather than intrusion.

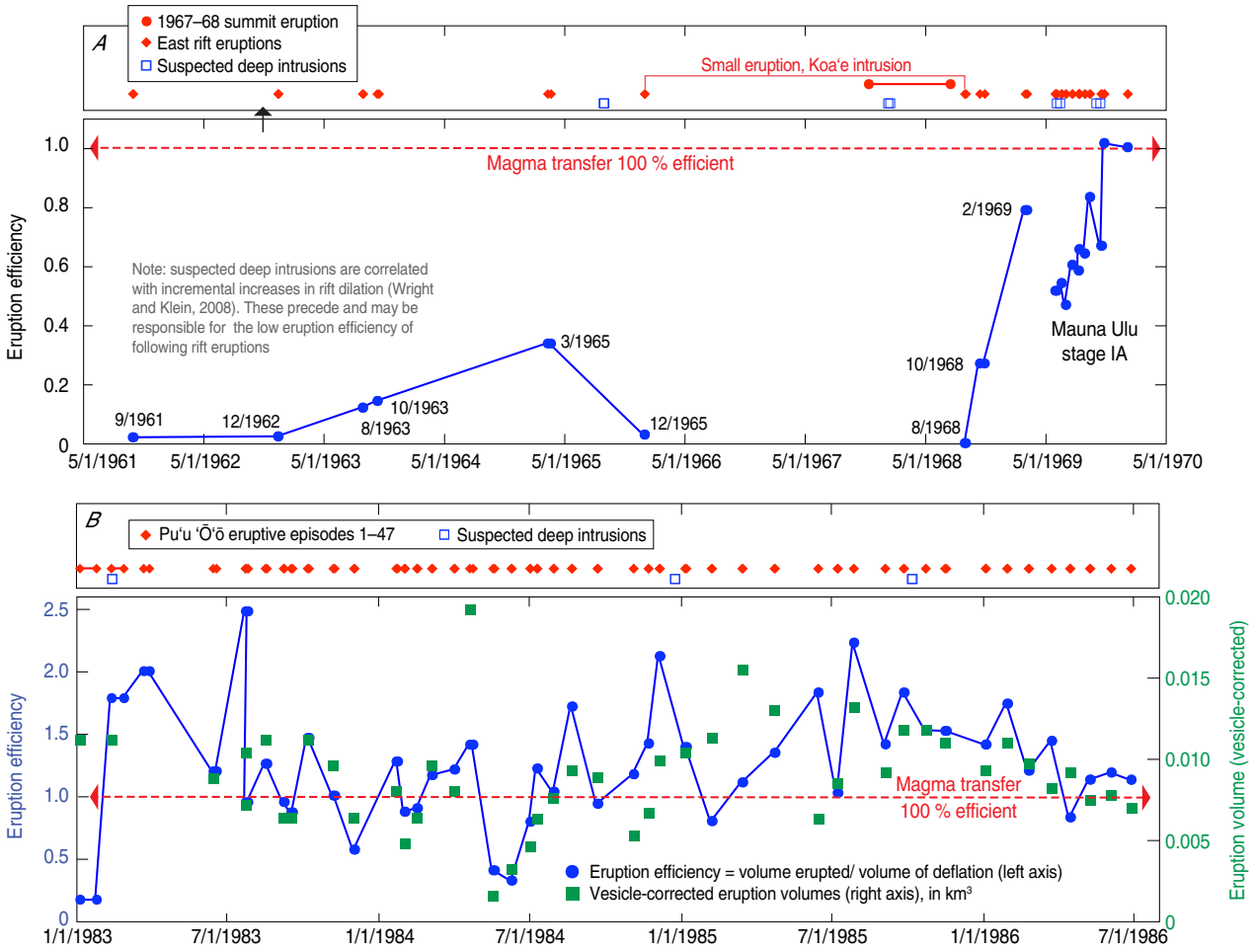

Figure 8.3. Graphs of Kīlauea eruption efficiency plotted against time. See text for further explanation. Dates on figure in m/d/yyyy format. ***A***, 1961–1970. Rift eruptions of the 1960s and Mauna Ulu Stage IA. ***B***, 1983–1986. Stage IA of the Pu‘u ‘Ō‘ō-Kupaianaha eruption. The vesicle-corrected eruption volumes used in the calculation of eruption efficiency are plotted to illustrate their great variability, largely a result of measurement uncertainty.

Traditional and Inflationary Intrusions as Related to Degree of Inflation

It makes sense than an inflated volcano has more magma at the ready to erupt or intrude. A broad view of the relation between frequency of intrusion and the state of inflation as measured by the daily record of the tiltmeter housed in the Uwēkahuna Vault is shown in figure 8.4. The frequency of traditional intrusions associated with tilt drops and a strong south-flank response is greatest at intermediate levels of inflation. Conversely, as the reservoir is filled and the volcano has reached a relatively high state of inflation, inflationary intrusions near the summit with little south-flank anticipation or response become dominant. This observation suggests that the reservoir can sustain high inflation only when intrusions are frequent and small. At these times we envision a full magma reservoir from which magma forces its way or "spills over" into the uppermost (near-summit) parts of the rift zones. Inflationary intrusions are thus more a measure of inflation than of magma supply or the stress state of the rifts.

Most periods of inflationary intrusions are followed by a major traditional intrusion that penetrates deeply into a rift zone. There is a quantitative link between inflation, as measured by high Uwēkahuna tilt values and by summit earthquake counts (Klein, 1982). Inflationary intrusions contribute to high summit earthquake counts. The inflationary intrusions of 1971 immediately preceded the seismic southwest rift zone (SSWR) eruption of 24 September 1971, and the inflationary intrusions of 1974 foretold the SSWR eruption/intrusion of 31 December 1974, as chronicled in chapter 5. The SSWR intrusion of June 1982 and east rift zone eruption of January 1983 were both preceded by episodes of inflationary intrusion. Exceptions exist to the general observation. The inflationary intrusions of January and February 1980 were not immediately followed by a large event, though the SSWR intrusion of February 1981 occurred 1 year later. The inflationary intrusions of January to March 2006 did not halt the Pu‘u ‘Ō‘ō eruption and did not enable a new intrusion, but when combined with the inflationary intrusion of May 2007, they may be causally related to the large Father's day intrusion of 17 June 2007, as chronicled in chapter 7. We therefore come to the important conclusion that the identification of inflationary intrusions, coupled with high summit tilt, indicates an increased likelihood of a major eruption or traditional intrusion.

The intrusion/eruption frequency is thus very sensitive to the inflation state, suggesting that the summit reservoir must be very sensitive to small changes in pressure. For example, tilt changes of about 100 μrad, corresponding to elevation changes of about 5 cm and a magma pressure increase of only 15 gm/cm^2, have a noticeable effect on intrusion frequency. On the other hand, an increase in the magma supply rate has only an indirect effect on the intrusion frequency, but it does promote inflation and increases the volume of magma available to sustain an intrusion.

A consequence of a finite magma supply within a given time period is that large-volume deflations will be followed by less frequent intrusions and a delay in the beginning of re-inflation. Major events that were not immediately followed by sustained inflation were the 1960 eruption and collapse, the 1975 Kalapana earthquake and collapse, and the 1983 Pu‘u ‘Ō‘ō eruption and collapse. These three major collapse events are among the largest in the 1960–2009 record and each may have effectively ripped a large opening in the reservoir that took years to heal until reservoir magma could be retained and major inflation resumed.

Magma Supply to Kīlauea

Magma Supply Rate

The magma supply rate is an important factor in evaluating the long-term history of any volcano. Its estimation is made inherently difficult by the great changes in the viscosity of magma with small reductions of temperature. Magma has to traverse an inhomogenous rock volume to reach the surface, and this may result in temporary delays in transport that may render meaningless all but the longest term estimates of supply rate. Figure 8.5*A* illustrates our best estimates of the rates of both rift dilation associated with south flank spreading (see discussion below) and magma supply over the past 90 years between 1918 and 2008. Figure 8.5*B* illustrates our best estimate of the increase in magma supply rate over the past 50 years. We have included reconstructed supply rates in green to match the reconstructed spreading rates shown in figure 8.6. Figure 8.5 also shows the short-term variability in estimated supply rate as illustrated for the period bracketing the Mauna Ulu eruption.

Magma supply rates before 1950 are estimated from eruption and caldera-filling rates assuming little or no south flank spreading or rift dilation. We infer that the high rates of magma supply and transfer associated with cycles of eruption, draining, and refilling before 1840 are a function of rebound from a massive draining of magma in 1790 that may be represented in Puna by 1790 lava and a possible accompanying intrusion. The 1790 eruption was not a caldera-forming event, but it did drain Kīlauea's entire magmatic system and triggered a very high rate of resupply through lowered pressure above the magmatic system. Filling rates before 1840 are

2–6 times those after 1840 (fig. 2.1). We interpret the decline in magma supply rate after 1840 to be in part a return to a low equilibrium rate and in part to result from the increased activity of Mauna Loa (see discussion below). The typical eruption rates from 1918 to 1924 are virtually the same as the average 19th-century caldera filling rate between 1840 and 1894 shown in chapter 2, figure 2.1.

The 1895–1918 magma-supply rate is difficult to estimate. The amount of magma needed to refill Halema‘uma‘u during the period from 1899 to 1918 is 0.0225 km^3, assuming filling of the frustrum of an inverted cone (chap. 2), yielding a filling rate of 0.0012 km^3/year, far less than in periods preceding and following. However, the filling shown in figure 2.2 is punctuated by (1) many disappearances of magma before continuous refilling began in 1907, (2) instances of magma withdrawal between 1908 and 1912, and (3) several deflations measured in the Whitney Vault and several drops of the Halema‘uma‘u lake level accompanied by earthquake swarms between 1912 and 1918 (fig. 2.3*A*). The south flank may have had active spreading during the first two decades of the 20th century, as suggested by the *M*6.7 flank earthquake in September 1908. If each of these categories of events (1–3 above) is interpreted as magma transfer to the rift zone, then we cannot disprove the null hypothesis that the actual magma supply rate was close to the 0.025 km^3/year estimated for the period before 1894 and after 1918 and was not seen as filling of Halema‘uma‘u lake[29].

We speculate that the low Halema‘uma‘u filling rate (as contrasted with a magma supply rate) during 1894–1918 (fig. 2.1) was related to the substantial regional caldera uplift of 1918–1919 seen on the Whitney tiltmeter (fig. 2.3*A*) and captured by Wilson’s (1935) 1912–22 leveling survey. It is as if the mantle magma supply was choked off at some depth in the upper mantle in the 1890s and was released in 1918 to replenish a large section of the supply conduit, including reservoirs 1, 2, and 3 and below them,

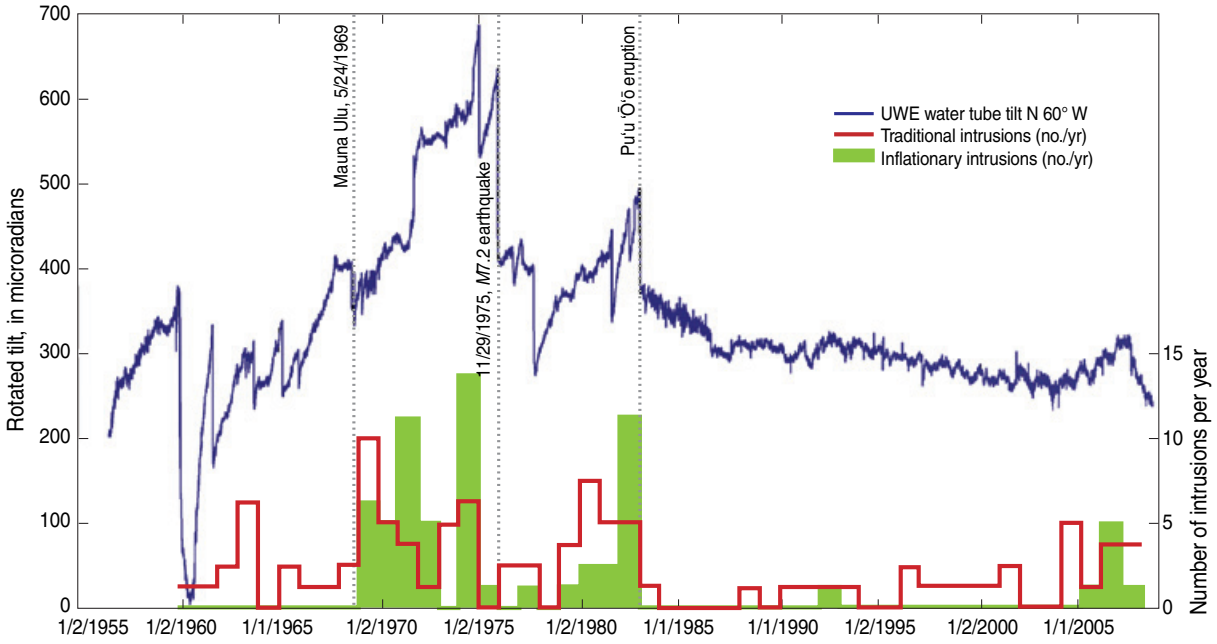

Figure 8.4. Graphs showing frequency of intrusion versus state of inflation at Kīlauea. The Uwēkahuna (UWE) water-tube tilt record is the best continuous measure of Kīlauea’s inflation and deflation after 1956. Because Uwēkahuna tilt measures the relative heights of two water pots anchored to the ground, this tilt has good long-term stability. The dashed vertical lines mark three major collapses discussed in this report. The offset caused by shaking during the *M*6.7 Ka‘ōiki earthquake on 16 November 1983 has been removed because it did not involve a magmatic change. Tilt is plotted as a single vector rotated to N 60° W., which points away from the typical inflation/deflation center and is a good measure of long-term inflation. Annual numbers of intrusions from event tables in previous chapters are plotted for traditional intrusions (red histogram) and inflationary intrusions (green histogram). Dates on figure in m/d/yyyy format. See text for interpretation.

[29]An alternative approach assumes that the magma supply during this 1894–1918 interval is equal to the bracketing values of 0.0249 km^3/year, then a maximum of 0.6 km^3 of magma entered the Kīlauea plumbing during that 24-year interval, of which 0.49 km^3 represents the volume needed to replenish the deep magma system (see fig. 2.1). Could the remaining 0.11 km^3 be accommodated in the east rift zone? Assuming a rift length of 30 km and height of the active rift zone of 2 km, the remaining 0.11 km^3 results in a rift extension of nearly 2 m over 24 years, or about half of the instantaneous opening observed following the 1975 earthquake (Owen and Bürgmann, 2006) and nearly twice the dilation rate calculated during the Pu’u ‘Ō’ō-Kupaianaha eruption (Owen and others, 1995, 2000a). There is no evidence from geodesy or seismicity for this much magma entering the rift and deforming the south flank during 1894–1918.

perhaps in the depth range of 2–30 km. This 1918 release of magma to shallower levels restored the caldera-filling rate and uplifted the caldera within a 4-month period. This charge of new magma provided a ready source for the 1924 east-rift intrusion and formation of the Kapoho dike, which also collapsed the summit back to its pre-1918 level and triggered the 1924 explosive Halema‘uma‘u eruption. The 1924 evacuation of magma from below the summit encouraged an approximate doubling of the magma supply (periods I to II, fig. 8.5*A*), and it certainly cleared any conduit obstruction that may have existed between 1894 and 1918.

Magma volumes and batches in the post-1950 era are ascribed to changes in magma reservoir 2, except for 1954 and 1959, which involved sources removed from the main plumbing (fig. 4.13). The volume calculations, combined with the observed 10-year time in which successive magma batches are recognized, can be used to estimate the minimum magma-supply rate between the arrival of the 1952 batch in 1950(?) and the using up of the 1967–68 batch in 1969. The total erupted volume is 0.51 km^3 (table 8.1), the total additional volume intruded beneath the east rift zone is 0.66 km^3 (table 8.1), yielding a magma supply rate of about 0.062 km^3/yr over the 19 year interval between 1950 and 1969, less than the magma supply rate of 0.086 km^3/yr estimated from the tilt calculations. This comparison is consistent with the addition to the rift zone of magma that passes through the summit reservoir but is not accessed by eruption to the surface. The aggregate volume of the 1967–68 magma batch exceeds the volumes of the two earlier batches, consistent with the increase in magma supply in the period following the 1967–68 eruption (fig. 8.5).

We conclude the following about Kīlauea’s historical magma supply: (1) The magma supply rate from 1840 to 1950 (<0.03 km^3/yr) was far less than what we observe from 1950 and after. (2) In the period between the 1924 collapse and the March 1950 inflation, the volume lost in the collapse was regained at a rate still uncertain. The net magma supply rate before 1950 must have decreased as the lowered pressure caused by the 1924 collapse was equalized, perhaps to a value equal to the 1918–24 filling rate. (3) Summit inflation, driven by increased magma supply, began when the volume lost in the 1924 collapse was recovered, possibly augmented by a shift in the deep mantle plumbing to favor eruption at Kīlauea over eruption at Mauna Loa (see below).

We interpret the 1950–75 period to be one of magma supply steadily increasing to a higher level typical of the rest of the century compared to the first two-thirds of the century (fig. 8.5). Kīlauea accomodated the higher magma supply through (1) more frequent rift zone eruptions and intrusions, including the prolonged 1969–74 Mauna Ulu eruption, (2) a stepwise increase in south flank spreading rate and seismicity, including suspected deep intrusions, (3) increase in the eruption efficiency, defined as the ratio of magma erupted to magma intruded, with continued use of the plumbing, and (4) shifts of the preferred rift zone from the east rift to the southwest rift and back again as the east-rift plumbing was unable to accommodate the magma supply (see chap. 5).

Magma supply rate continued to increase incrementally following the beginning of continuous east rift eruption in 1983. We accept a value of 0.18 km^3/yr in stage I, increasing to 0.2 km^3/yr in stage II following the 1997 eruption and intrusion. Magma supply increased further during stage III following the shift from deflation to inflation at the end of 2003 and the 2.5-fold increase in CO_2 emission in 2004–2005. Poland and others (2012) have suggested that events after 2003 were driven by a surge of deep magma supply that released CO_2 with time delays between (1) the surge and the measured CO_2 increase and (2) between the CO_2 increase and the shallow manifestations of increased magma supply mentioned in chapter 7. In their estimation the Father’s Day eruption in 2007 and the connection of the magma transport path beneath Halema‘uma‘u to the surface in 2008 were driven by a minimum 2-fold increase in magma supply. We incorporate their estimates into figure 8.5, while questioning whether ground deformation and seismic data coincident with the time of CO_2 increase support that magnitude of magma supply increase. Finally, these authors estimate that magma-supply rates gradually returned to pre-2003 levels following the 2008 Halema‘uma‘u eruption that ends our study.

Magma Storage and Pathways

The primary summit magma reservoir at 2–6 km below the caldera (fig. 8.1) is not the only one active since the founding of HVO in 1912. The sharp deflation in 1924, associated with an explosive Halema‘uma‘u eruption and an east-rift eruption and intrusion, is correlated with large draining of the lava lake and is consistent with draining magma reservoirs 1 (0.8-km depth), 2 (3.5 km), and 3 (fig. 2.4). Levelling implicates draining of reservoirs at three depths, and the involvement of the deeper reservoir 3 in a summit collapse is unique in the deformation record (see chap. 2). The Whitney tilt record shows an increase in 1918–19 and subsidence in 1924–25 that are consistent with Wilson’s (1935) initial conclusion of a 1-foot increase in the altitude of the Volcano House benchmark before the 1921 triangulation and an even greater decrease in altitude across the 1924 collapse. The 1912–22 rise and 1922-27 fall of the

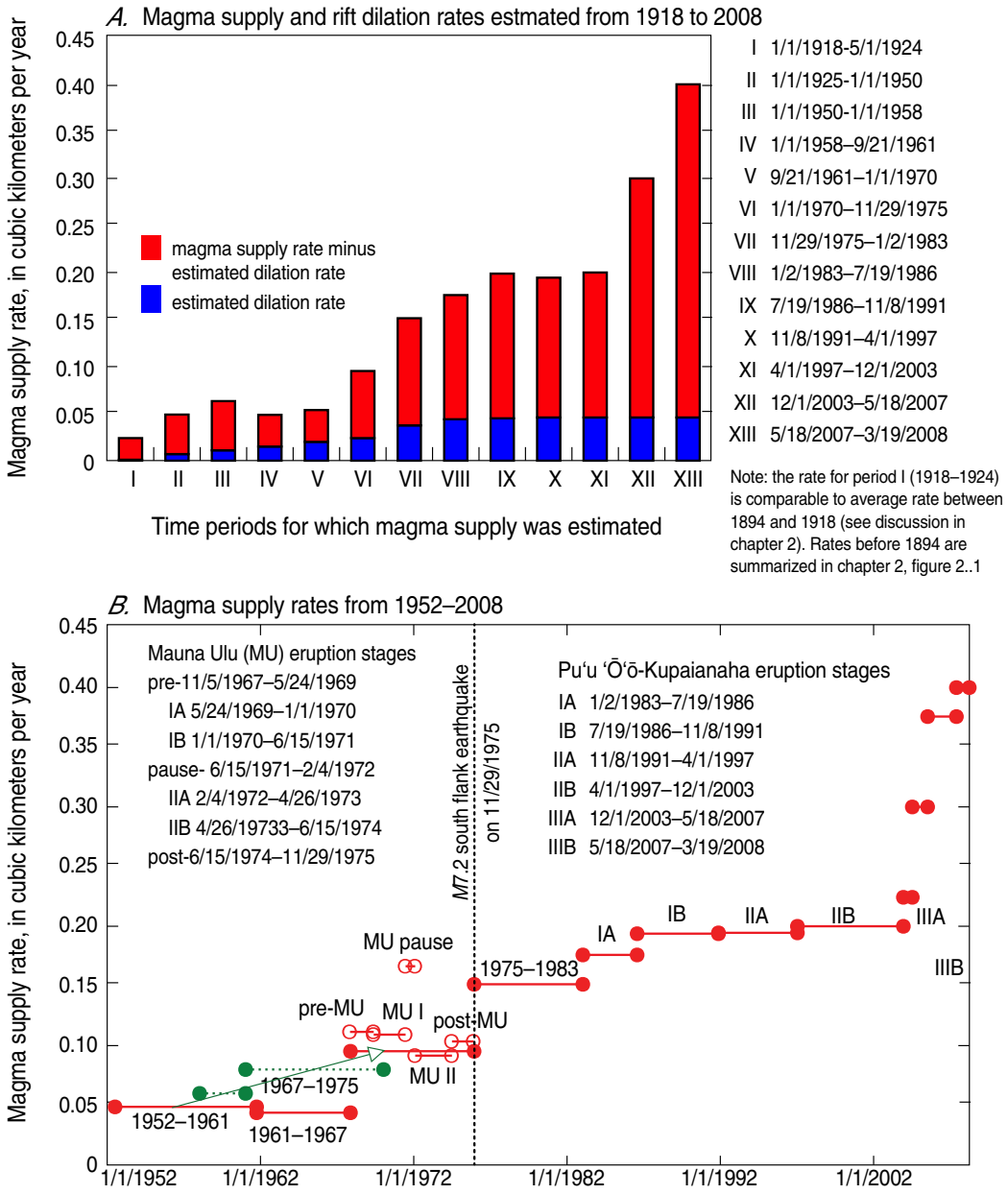

Figure 8.5. Graphs showing long-term rates of magma supply and rift dilation at Kīlauea. Dates on figure in m/d/yyyy format. ***A***, Magma-supply and estimated east-rift dilation rates for the period 1918–2008. For periods before 1950, magma-supply rates are equated to magma filling/eruption rates because the rift dilation (spreading) component is unknown and assumed to be close to zero. The eruption rates from 1918 to 1924 are virtually the same as the average 19th century caldera filling rate between 1840 and 1894 (chap. 2, fig. 2.1). After 1950 magma-supply rates are calculated using the sum of volume-equivalents of deflations at Kīlauea's summit as shown in tables in previous chapters. During long eruptions, the eruption volume is added to the tilt volumes. Dilation rates are assumed between 1950 and 1975. The 1975 Kalapana earthquake had a dilation volume of 0.4 km^3 (Owen and Bürgmann, 2006). Dilation during the eruption that began in 1983 is about 0.0459 km^3/year (Owen and others, 2000a). ***B***, Magma-supply rates from 1952 to 2008. Over the long time span, magma-supply rates increase. Over shorter periods of time, the magma supply calculated as above is quite variable, as illustrated by the various stages of the Mauna Ulu eruption. Individual magma-supply rates have associated errors of about ±20 percent. The green arrow spanning intervals before 1972 indicate increases in magma supply rate that match the increases in south flank spreading rate shown in figure 6.6*A*. A 2.5-fold increase in CO_2 from Kīluaea's summit begins in stage IIIA; decline is gradual after mid-2005. Magma supply increases to 2008, then decreases, following the increase and decrease of CO_2, as indicated by M. Poland and J. Sutton (oral and written commun., 2010). Magma supply rates after the beginning of inflation in 2003 are estimated by Poland and others (2012) and are applied to both 8.5*A* and 8.5*B*, although we remain skeptical as to whether the increase in magma supply was as great as would be suggested by using summit CO_2 emission as a proxy for magma supply rate (Gerlach and others, 2002).

Kea‘au benchmark argues that its change is due to inflation and deflation of a deep magmatic source.

The events of the 1953–60 period stand apart from the rest of Kīlauea’s recorded history. The deep (40–60 km) seismicity during 1953–60 and the unique chemistry of the 1959 Kīlauea Iki eruption strongly suggest that the magma being supplied was from an alternate deep mantle source above the normal Hawaiian mantle source and that movement of magma from this source to the surface did not follow the typical magma conduit feeding Kīlauea’s shallow reservoir—rather, it made a unique path toward Kīlauea Iki (see chap. 4). We thus think of the deep Kīlauea conduit as being multistranded (Wright and Klein, 2006, figure 10 and discussion, p. 63–64).

South Flank Seaward Spreading

Seaward spreading of Kīlauea’s south flank is an essential complement to the history of the volcano’s magma supply. Spreading is associated with dilation of the rift zones, thus creating additional room for magma to occupy. The south flank has been described as a stress meter whose seismicity responds to changes in rift stresses and magma pressure (Dieterich and others, 2000). Continuous seaward spreading has been documented by numerous triangulation, EDM, and GPS campaigns and recently by continuously recorded GPS stations. It is our assumption that some degree of spreading and rift dilation are essential for eruption (or intrusion) on the rift zones. Construction of a summit shield, such as the ‘Ailā‘au shield (Clague and others, 1999), probably can occur only when the rift zones are sealed. In this section we address the question of spreading and its relation to eruption and intrusion in terms of the long term history of ground deformation measurements and south flank seismicity.

History of Seaward Movement of Kīlauea’s South Flank

The history of Kīlauea’s south flank moving southeast away from Mauna Loa is shown in figures 8.6*A*–*C*, and the differential movement within the lower south flank is shown in figures 8.7*A*–*C*. The south flank data were obtained by four different methods. The results of the earliest triangulation studies extending from 1896 or 1914 to 1970 are summarized and interpreted by Swanson and others (1976a). We plot their data, but make an adjustment to the long period separating 1914 and 1958 in order to postulate an increase in spreading rate beginning with the reinflation of Kīlauea in March 1950 (fig. 8.6*A*). Later, the higher magma supply may have triggered the offshore south flank earthquake swarm of March and April 1952. We interpret the offshore swarm to have unlocked the south flank, potentially marking the beginning of much less constrained seaward spreading. Subsequent to 1961, horizontal displacements were obtained by EDM (1965–89), campaign GPS (1989–96) and continuously recording GPS (1996–present). Station locations and measured displacements are stored in a computer database (VALVE) maintained by the U.S. Geological Survey’s Hawaiian Volcano Observatory (HVO). GPS data were first published in papers by Paul Delaney and others and by authors cited therein (Delaney and others, 1993, 1998). Paul Segall and students of his have collaborated with HVO personnel to continue measurements during the eruption that began in 1983 (see, for example, Owen and others, 1995, 2000a).

It is difficult to compare directly the pre- and post-EDM periods because the EDM network was occupied less frequently than the subsequent GPS network. As GPS stations were installed, EDM stations were replaced or abandoned for a variety of reasons, and the GPS networks were not always colocated with the older EDM networks. For these reasons it is difficult to construct a single south-flank movement curve. Displacement measurements during the Mauna Ulu eruption are incomplete. Data published in the two papers cited above cannot be compared, because the Delaney paper shows detailed measurements of seaward movement of the entire upper south flank, whereas the Swanson paper by contrast shows detailed measurement of movement within the lower south flank (figs. 8.6*B*, 8.7*B*).

Nonetheless it is possible to make some broad comparisons between gross flank motion and internal compression. There is an obvious offset at the time of the 1975 earthquake, with distances lengthening both from Mauna Loa to the south flank (fig. 8.6*A*) and within the south flank (fig. 8.7*A*). Another striking change is the slowing of south-flank spreading rates at the beginning of the Pu‘u ‘Ō‘ō-Kupaianaha eruption (fig. 8.6*A*). At the start of that eruption in 1983 there is a slowing of flank compression within the lower south flank (figs. 8.7*A*,*C*), as documented by Delaney and others (1998), and a possible weak reversal to slow extension after 1997 (fig. 8.7*C*). Since 1983, the south flank motion has been more or less constant at 5–6 cm/yr, with the exception of a small offset accompanying the 1997 intrusion (fig. 8.6*C*). The larger slow-slip events (Montgomery-Brown and others, 2009), discussed in a subsequent section, are apparent in figure 8.6*C* as net south flank motion if two measurements made days apart span the event. Slow-slip events are too small to appear as internal flank extension on figure 8.7*C*, except for the 2007 Father’s Day event. Overall, these slow-slip events have only a small effect on the yearly motion.

South-flank motion during the 1969–74 Mauna Ulu eruption can be interpreted volcanologically. The low rate of seaward movement of the upper south

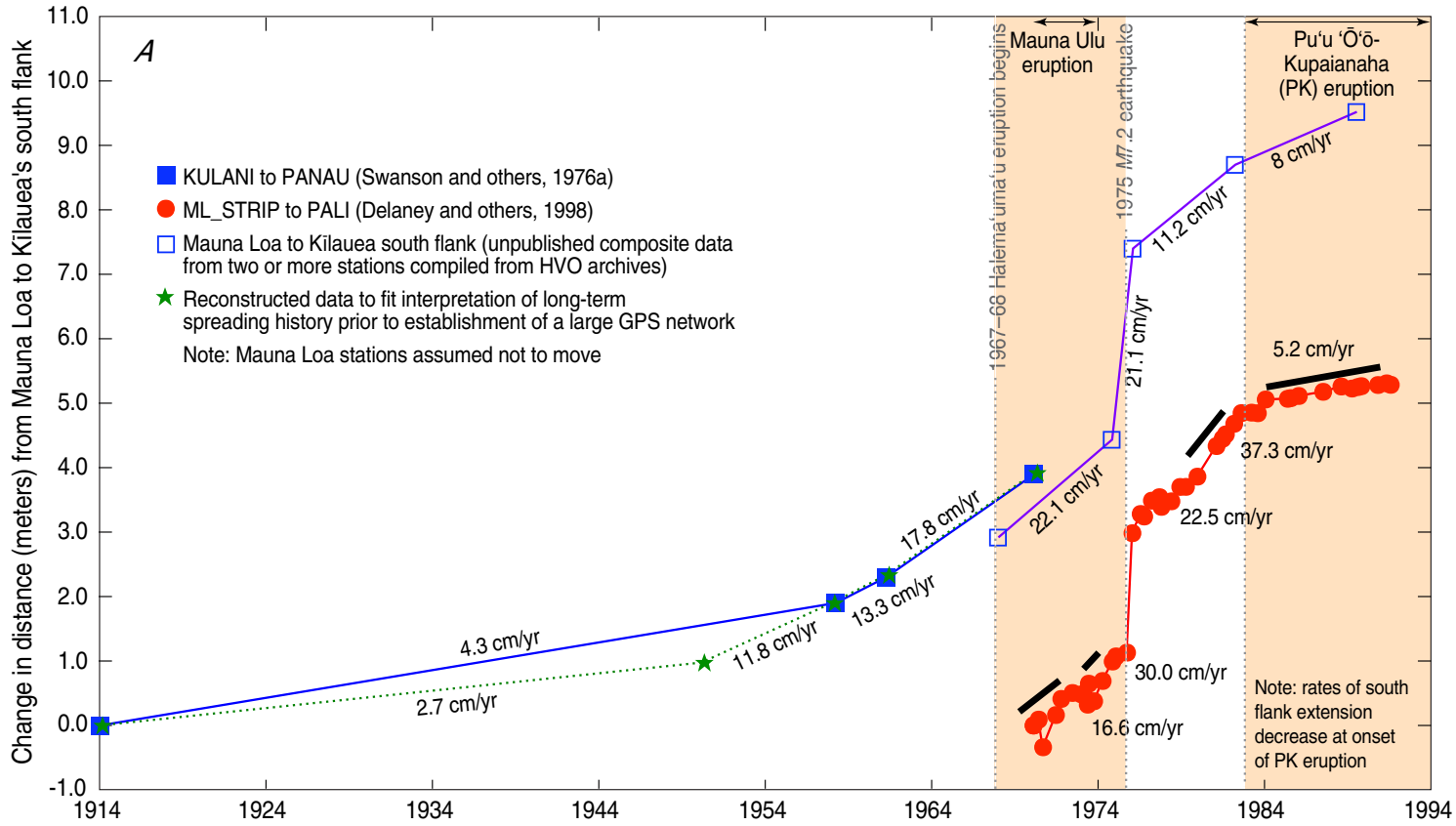

Figure 8.6. Graphs showing seaward movement of Kīlauea's south flank away from Mauna Loa's south flank, which is assumed stable. Station locations are shown in appendix figure H1. ***A***, 1914–1992: Data points shown by blue squares are from triangulation (Swanson and others, 1976a, fig. 5). Data points shown by red filled circles are from electronic distance-measuring (EDM) data from the EDM line connecting the Mauna Loa strip road station ML_STRIP with the Kīlauea station PALI, located on the northern south flank just south of the Koaʻe Fault Zone (Delaney and others, 1998, fig. 2b). The latter dataset shows significant extension at the time of the 1975 earthquake, a high rate of extension following the earthquake, and a significant drop in rate after the beginning of the Puʻu ʻŌʻō-Kupaianaha eruption in 1983. Data points shown by hollow purple squares are unpublished data from the Hawaiian Volcano Observatory files. Green stars show a suggested reconstruction of the deformation history consistent with both the observed data and the analysis of spreading presented in this paper. ***B,*** From 1 May 1969 to 1 July 1974: Data on the length of the EDM line ML_STRIP to PALI gathered during part of the Mauna Ulu eruption and shown at an expanded scale, with Kīlauea eruptions and intrusions for the same time period. See text for interpretation. Dates on figure in m/d/yyyy format. ***C,*** From 1982 to 2008: Lengthening of lines connecting Mauna Loa's south flank (assumed to be stable) with stations located near the coast on Kīlauea's southern south flank. Also shown are Kīlauea eruptions and intrusions for the same time period. Measurements are made by EDM (blue squares) and by Global Positioning System (red filled circles and green triangles). Station locations are shown in appendix figure H1. The dotted line is a suggested reconstruction across a large time gap in the data to reflect extension at the beginning of the Puʻu ʻŌʻō-Kupaianaha eruption and a slowing of the extension rate thereafter. Extension rates have remained near-constant during the long eruption, with the exception of small extensions recorded at the times of major east rift intrusions and silent earthquakes.

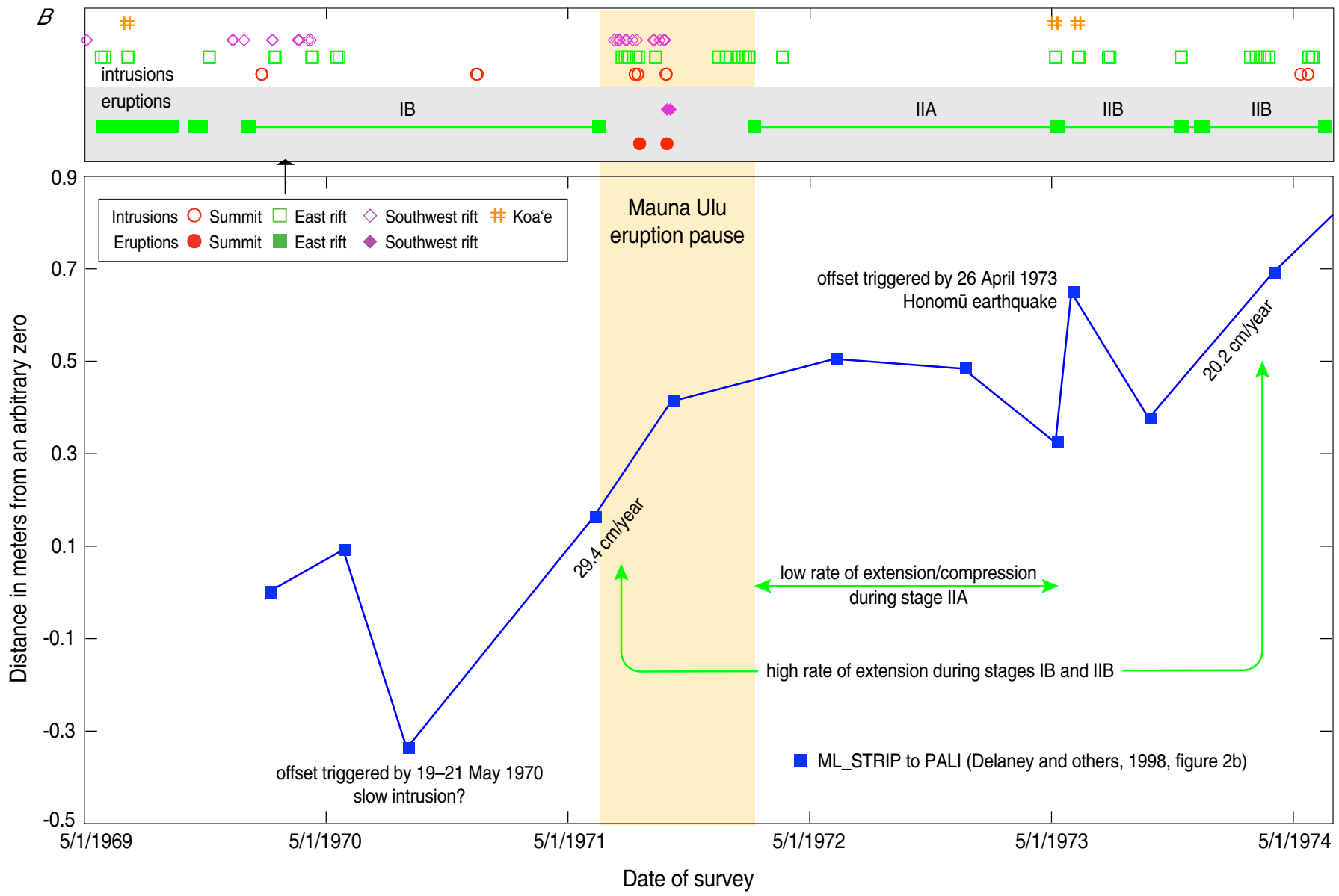

Figure 8.6.—Continued

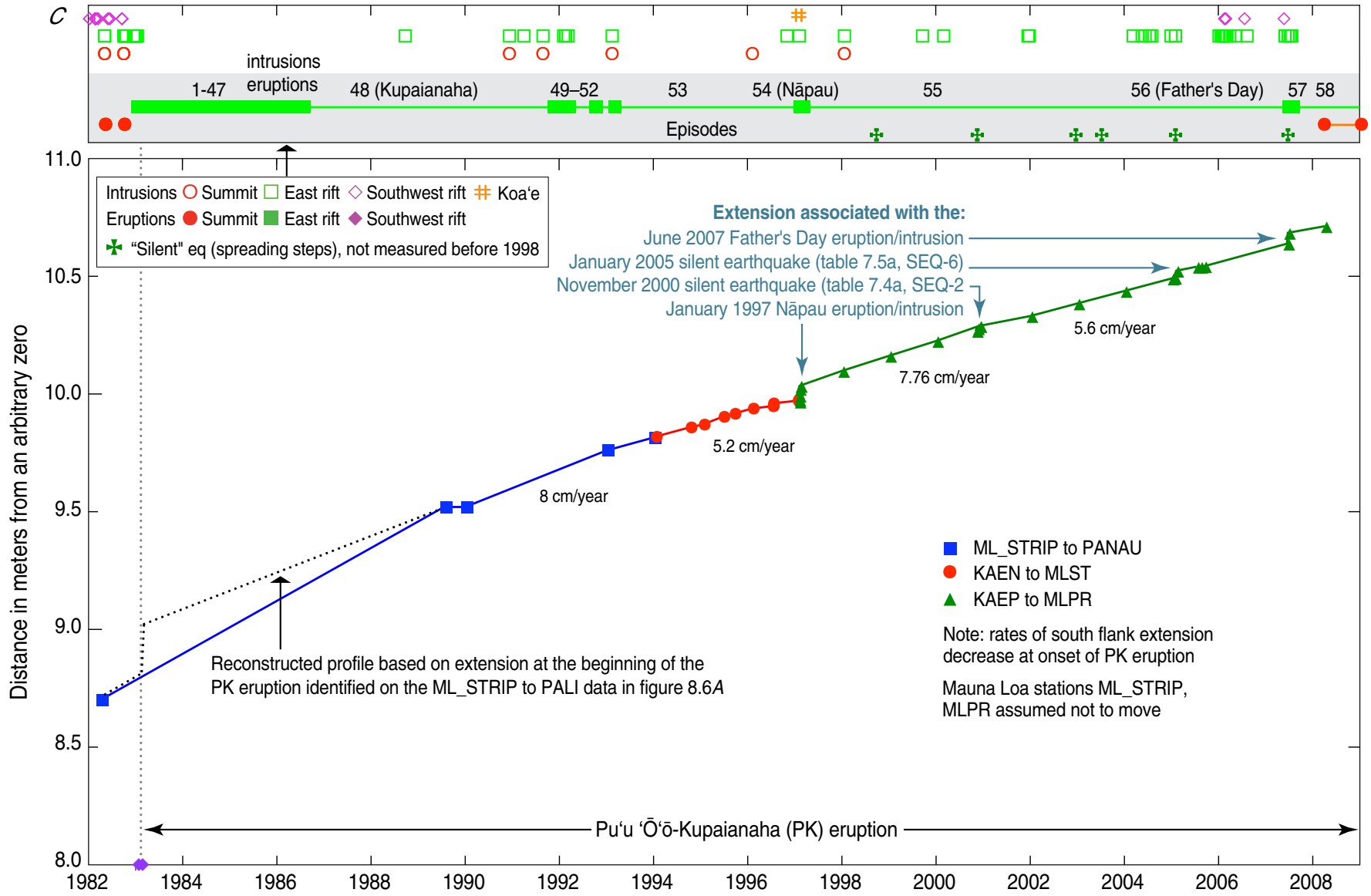

Figure 8.6.—Continued

flank during stage IIA (fig. 8.6*B*) is consistent with our interpretation that this was a period of equilibrium between magma supply and eruption rate as evidenced by summit deflation and low seismicity. The higher rates of flank motion during stages IB and IIB are consistent with our interpretation of increased magma pressure represented by inflation and higher seismicity. Unfortunately the only data available in this period are for the northern south flank, whereas post-1980s spreading rates are measured using south flank stations near the coast.

Line length changes that occur within the south flank are much more difficult to interpret in terms of spreading away from Kīlauea's stable north flank. Internal changes depend both on flank motion and on stresses applied to it. Change of line lengths within the lower south flank (fig. 8.7*A*) show compression between the 1975 earthquake and the beginning of the Pu‘u ‘Ō‘ō-Kupaianaha eruption, shifting to much smaller amounts immediately after the beginning of eruption. We interpret the compression before 1983 as a result of magma added to the rift while the south flank block was buttressed offshore and at its base. We see the extension after 1983 as a release of south flank stress and compression as magma was erupted from the rift. This release of compressive stress at the time of the 1983 eruption was seen by as a fivefold decrease of the stress rate within the south flank (Dieterich and others, 2003). After 1988 the lower south flank varies between extension and compression at much smaller within-flank rates of less than 1 cm/yr (fig. 8.7*C*).

The seismicity of the south flank offers clues to its stress state in addition to its internal compression seen both before and after the 1975 Kalapana earthquake. The Kalapana earthquake profoundly altered stress on the south flank and "softened" it to the stress imposed by magma traversing the east rift. After the earthquake, intrusions outnumbered eruptions, so it was more difficult for magma to experience enough confining stress to reach the surface, whereas before the earthquake, the opposite was true. The high rate of aftershocks in the 17 years following 1975 means the stress released by the mainshock was large, but the relatively high rates of seismicity in the south flank even before the earthquake also means that the stress rate on the flank actually decreased at the time of the earthquake (Klein and others, 2006). This lowering of stress rate in 1975 means that the large number of postearthquake east-rift intrusions without the magma pressure release of long eruptions (like Mauna Ulu 1969–74 and Pu‘u ‘Ō‘ō 1984–2014 ongoing) was offset by a softened and pliable flank such that the internal compression rates before and after the earthquake were about the same (fig. 8.7*A*).

Changes before the Mauna Ulu eruption show compression at a low rate through the 1967–68 summit eruption, a higher rate through the three 1968–69 east rift eruptions that preceded Mauna Ulu, then a return to a low compression rate during stage IA and variable rates during stage IB, when many more measurements were made (fig. 8.7*B*). The small changes during stage IB are difficult to interpret in the absence of measurement of other station pairs.

South Flank and Summit Tilt Response to Eruptions and Intrusions

The south flank responds to magma pressure applied over a range of depths beneath the rift zones. Earthquake swarms beneath Kīlauea's south flank often precede by minutes to days before, and usually follow in the days after, traditional eruptions and intrusions, and also after some inflationary intrusions. Time relations among the beginning of eruptions and earthquake swarms beneath the summit, rift zones, Koa‘e, and south flank are tabulated in the opening table of each of chapters 4–7, along with the response of a continuously recording tiltmeter at Kīlauea's summit. Of particular interest is the triggering of south flank earthquake swarms minutes to days ahead of earthquake swarms in the regions where eruption or intrusion occurs. Figure 8.8*A* shows for selected traditional eruptions and intrusions the time elapsed between triggering of an earthquake swarm beneath the south flank and the beginning of a shallow earthquake swarm within the rift. The rift swarm indicates that rock is breaking to initiate formation of a dike before eruption or intrusion. Note that south flank activity preceding intrusions may begin with a few small flank earthquakes hours before the intrusion, and the intrusion will generally trigger a much greater flank response lasting days afterward. Thus the south flank is responding to stress imposed by magma emplaced at a variety of depths within the rift both before and after the intense dike-forming swarm within the rift.

The time delay between flank and rift earthquakes varies. In rare cases, as during the large rift intrusion/eruption in September 1961, the south flank responded seismically only several hours after the beginning of eruption (table 4.1). This may have been because the intrusion was in a part of the rift zone not active for decades, or may have been a function of the limited seismic network at that time when it was difficult to clearly separate earthquakes beneath the rift zone from earthquakes beneath the adjacent south flank. Subsequent time delays between rift and flank earthquakes for intrusions beneath the east rift zone have all been shorter than the 1961 delay. Movement of magma in a shallow (0–4 km) dike can be initiated as a response to the pressure of incoming magma applied to the deep magmatic system. We have no evidence that magma moves upward from the deep rift to feed the shallow intrusion, but only that many

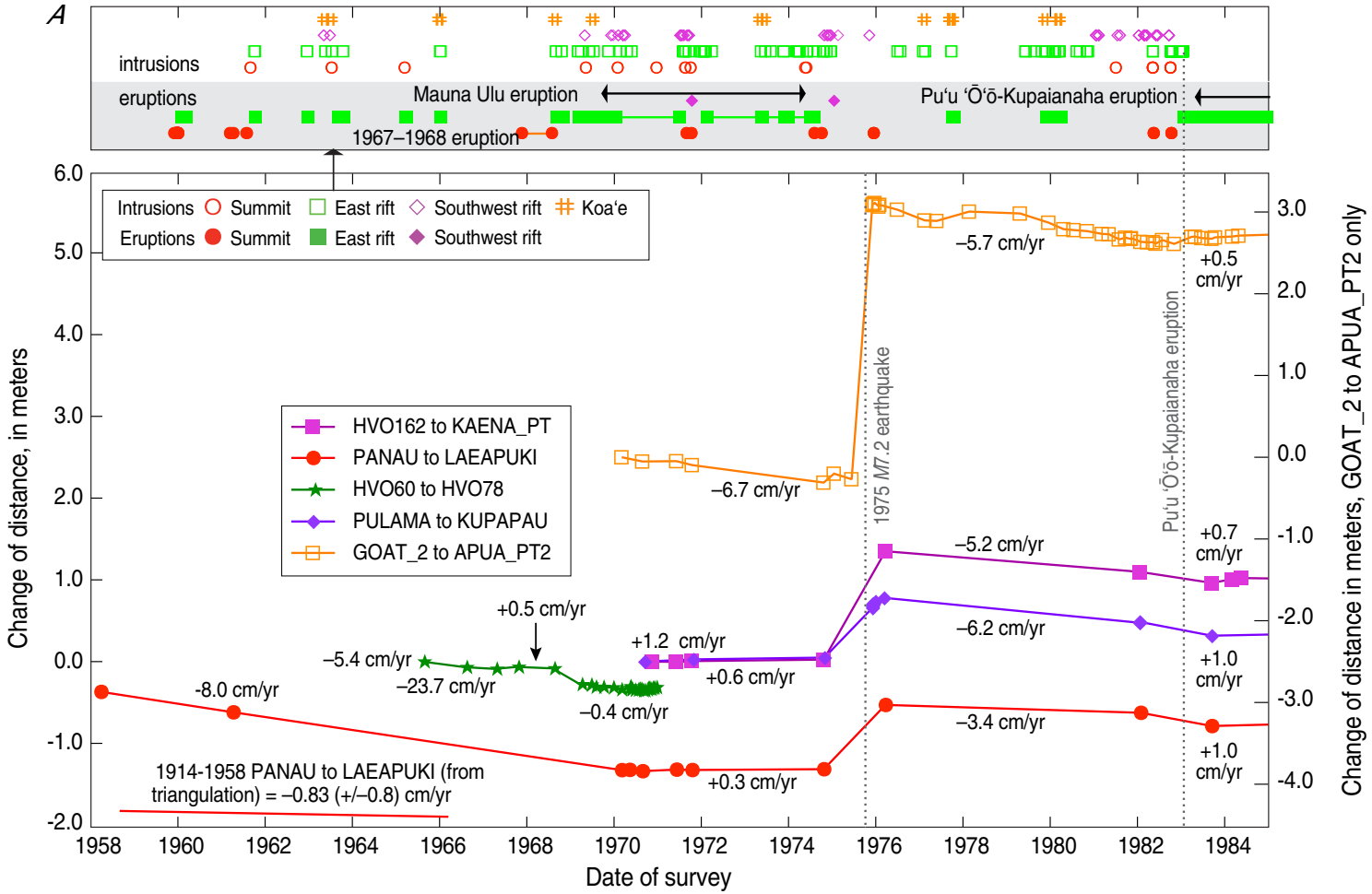

Figure 8.7. Graphs showing changes of line length between stations all located within Kīlauea's south flank. Station locations are shown in appendix figure H1. ***A***, 1958–1985. Line lengths within the near-coast south flank decrease up until the Mauna Ulu eruption, increase slightly till the 1975 earthquake, increase across the earthquake, decrease following the earthquake, and increase slightly following the beginning of the Pu'u 'Ō'ō-Kupaianaha eruption. One line, from the northern south flank GOAT_2 station to the coast APUA_PT2 station, shortens during the time before the 1975 earthquake, in contrast to the other station pairs. See text for explanation. ***B***, 1965–1971. A single pair of stations on Kīlauea's southern south flank was measured repeatedly during part of the Mauna Ulu eruption. It shows shortening before the 1967–68 Halema'uma'u eruption, little change during that eruption, a higher shortening rate before the beginning of the Mauna Ulu eruption, and small changes during the eruption. See text for explanation. ***C***, 1982–2008. History of line-length changes within the southern south flank using several different Global Positioning System (GPS) lines. The data show shortening across the beginning of the Pu'u 'Ō'ō-Kupaianaha eruption, partial recovery and further lengthening through Stages I and IIA, slight lengthening during Stages IIB and IIIA, and shortening and partial recovery during and after the Father's Day eruption. Numbers in top panel refer to episodes of the Pu'u 'Ō'ō-Kupaianaha eruption. See text for further explanation.

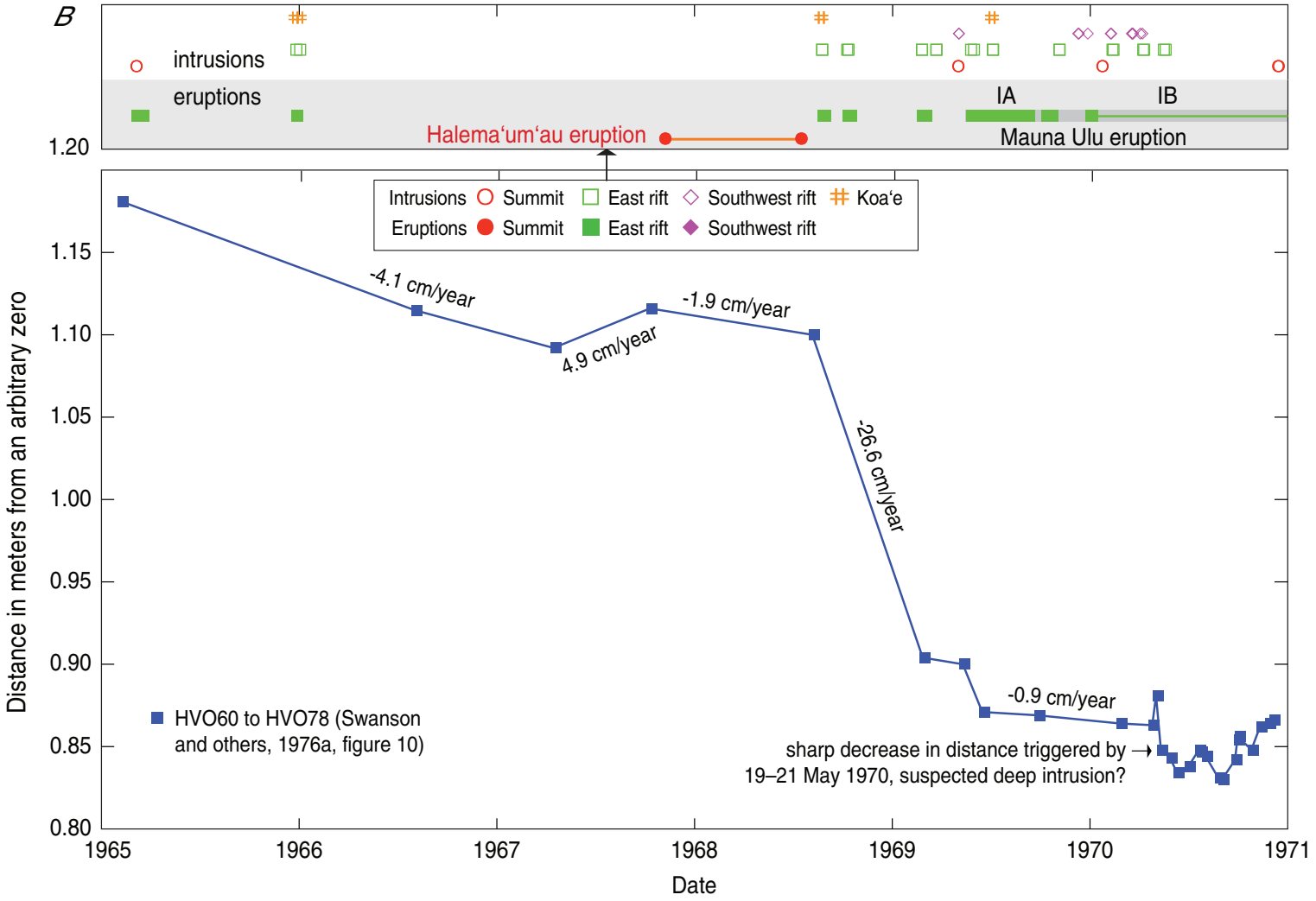

Figure 8.7.—Continued

rift intrusions begin as increased pressure applied to deep rift magma system is manifested in south flank seismicity before the shallow rift dikes expand. The south flank earthquakes (typically 5–9 km deep) are also a direct response to movement of magma into the deeper rift zone. The south flank thus behaves as both an early warning of and later response to increased magma pressure applied beneath the rift zone.

An additional argument suggests that south flank earthquakes that are precursory to rift intrusions respond to magma movement deeper in the rift at 4–10 km, as evidenced by flank seismicity near and downrift of the eruption site and new dike location. One would generally expect rift pressurization only uprift of the eruption site as magma approaches the eruption site. The observation of deeper flank seismicity near and downrift of the eruption site suggests that magma is expanding a deeper part of the rift surrounding the future dike site, and this magma may help to feed the dike from several directions at once.

The seismic southwest rift zone (SSWR) behaves differently to intrusions from the east rift because the flank response may be 1–3 days late. For three large events in September 1971, December 1974, and August 1981 (fig. 8.8*A*) the south flank massively responded hours to days following the initiation of an earthquake swarm beneath the rift, in addition to minimal south flank seismicity preceding the intrusion. It may be that, with less frequent use, the flank adjacent to the SSWR is lightly stressed by the rift to keep up with ongoing flank spreading. Alternatively, the flank adjacent to the SSWR may be "softer" and may require the intrusive stress to be applied for a longer time to achieve south flank slip.

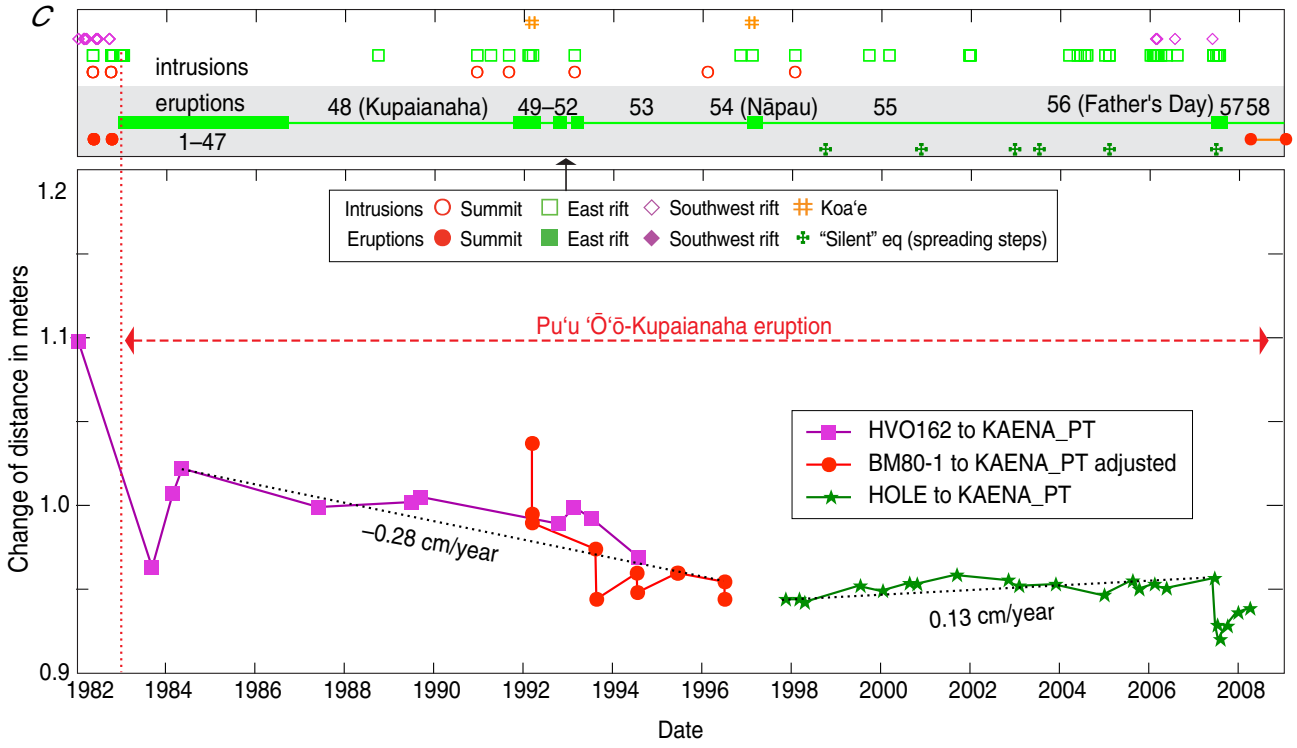

Figure 8.7.—Continued

The continuous summit tilt dataset affords an insight into the nature of resupply of magma from the summit magma reservoir to eruptions on the rift zone (fig. 8.8*B*). For most eruptions, the tilt deflection occurs after the beginning of an earthquake swarm marking eruption or intrusion. This indicates that most rift eruptions are initially fed from magma already stored beneath the rift zone and that the summit reservoir replenishes magma to the rift, a conclusion previously documented in some detail in chapter 6 of the present report and also previously (Klein and others, 1987). A notable exception is the December 1965 eruption, in which the Koa'e Fault Zone underwent significant deformation, and the short eruptions of 1979 and 1980 during the period of recovery from the 1975 earthquake. In these three instances, supply of magma from the summit can be interpreted to have destabilized the Koa'e Fault Zone in 1965 and caused unsustainable eruptions to occur in 1979 and 1980 when magma might have been expected to remain underground as an intrusion.

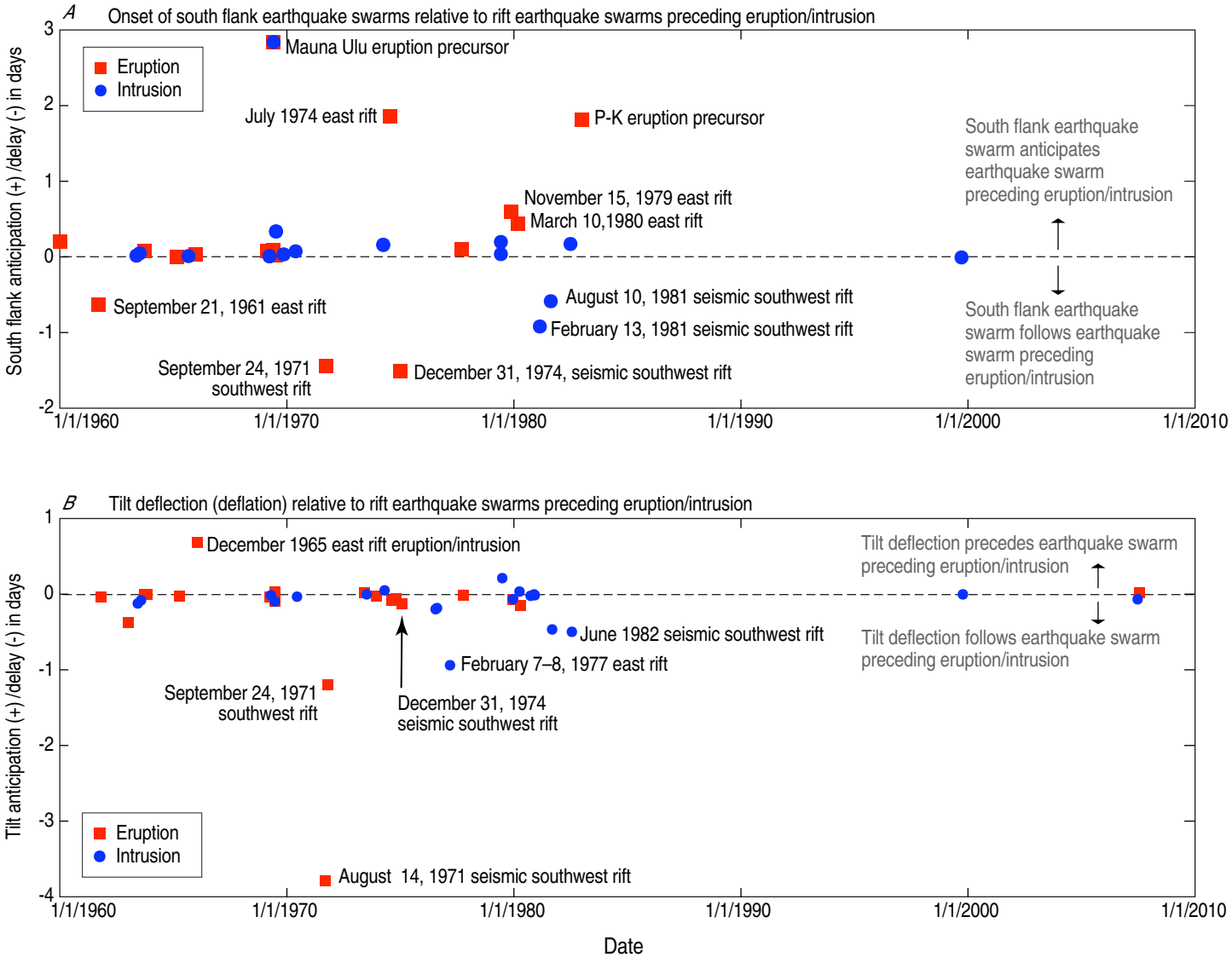

Figure 8.8. Comparison of onset times of Kīlauea earthquake swarms and the beginning of intrusions or eruptions or deflation at Kīlauea's summit. Dates on figure in m/d/yyyy format. ***A***. Comparison of onset times for rift and south flank earthquake swarms. For most intrusions and eruptions on the east rift, earthquake swarms beneath the south flank precede by minutes to hours earthquake swarms beneath the east rift. For a few large events, such as intrusions in July and December 1974, the south flank anticipation exceeds one day. For intrusions on the seismic southwest rift, earthquake swarms beneath the south flank follow the onset of an earthquake swarm beneath the rift zone with a delay of many hours. ***B***. Comparison of onset times for rift earthquake swarms and summit deflation. For most eruptions and intrusions, the onset of an earthquake swarm beneath the rift precedes the beginning of summit deflation by minutes to hours, as measured by a continuously recording tiltmeter in Uwēkahuna Vault. This is consistent with the idea that rift intrusions sprout from zones where magma has been previously stored. For intrusions on the seismic southwest rift zone, the delay may be as much as several days. An exception is provided by the December 1965 eruption/intrusion into the Koa'e Fault Zone, in which the onset of rift seismicity followed the beginning of summit deflation by several hours, suggesting that pressure from magma moving from the summit reservoir was instrumental in opening the Koa'e.

History of Located Earthquake Counts and Seismic Moment Accumulation

The long-term seismic history complements and supports the long-term study of magma supply and south flank spreading. Earthquake counts are difficult to compare before the completion of a comprehensive network and processing facilities in the early 1970s, and even after 1970 their numbers are still subject to variation in the completeness and nonuniformity of small-magnitude earthquakes. In our study we have distinguished short period (SP) and long period (LP) earthquakes, the latter designated in the catalog only after 1972; both are related to stresses from magma flow, but LP earthquakes are more intimately associated with magma conduits. Moment accumulation is dominated by the largest earthquakes, all of which are short-period, and these therefore offer a more reliable comparison of stress.

Seismicity Variation over Intervals of Time

We focus first on short-period seismicity to broadly compare the changes over large periods of time as shown in figures 8.9 (chaps. 4, 5 and 6; 1950–82) and 8.10 (the Pu‘u ‘Ō‘ō-Kupaianaha eruption period of chap. 7; 1982–2008). Earthquake counts include all located earthquakes regardless of magnitude and show the effects both of seismic network improvement and relative seismicity values within periods of stable earthquake processing. Seismic moment, however, is determined by the largest earthquakes and is not affected by increases in small event completeness in this post-1950 period. Moment accumulation in all regions is shown for the period from 1950 to 1982 (fig. 8.9*B*) and for comparison the time period encompassing the eruption that began in 1983 (fig. 8.10*B*). Figure 8.9*A* shows the effects of improved detection of located earthquakes in all regions, particularly in 1969–70, and the 1969–82 values are higher because of this. The central south flank (sf 2.3) dominates both in counts and moment in nearly all time periods. High moment values in figure 8.9*B* are primarily determined by the large-magnitude earthquakes listed. Particularly noticeable is deep magma-supply seismicity (region ms 4.5), which increased beginning in 1961 after the reinflation of Kīlauea in 1950 and continued to be elevated up to the time of the 1975 earthquake.

The period following the 1975 earthquake is dominated by its aftershocks in the south flank regions. We have tried to minimize the effect by beginning this period on 1 January 1976, after the majority of aftershocks had ocurred. Particularly noticeable in this period is the sharp decline in the rate of deep magma-supply earthquakes, probably because stress on this zone was relieved by south-flank slip directly above, which has the same faulting mechanism (Klein and others, 1987). East rift seismicity and, to a lesser extent, seismic southwest rift seismicity increase as a function of the many intrusions occurring in this period.

The period after 1982 and particularly after 1986 shown in figure 8.10 shows greatly decreased seimicity in all regions following episode 1 of the Pu‘u ‘Ō‘ō-Kupaianaha eruption. Seismicity is higher in the period preceding the 1997 east rift intrusion and preceding the Father’s Day eruption (stages IIA and IIIA). Overall, the rate of moment release is far below that of the periods preceding the 1975 earthquake.

Continuous Seismicity Variation

Continuous variation in cumulated seismic moment for short-period earthquakes in all regions is shown for the periods between 1950 and 1975 (fig. 8.11) and between 1983 and 2008 (fig. 8.12). We seek in these and succeeding figures to determine changes in strain release over time and correlate it with the magma supply and south flank spreading history. We assume that earthquake moment rates generally increase with magma flow rates, though we cannot verify this quantitatively or statistically. We are also aware that some seismicity deeper than 20 km is related to lithospheric flexure (Klein and Koyanagi, 1989), and we suspect that earthquakes classified as "deep magma supply" may act as a stress trigger when added to the much larger stress imposed by the volcanic load on the oceanic lithosphere. We look at changes of rate (slope) in different regions to better understand how the volcano responds to magma transport and storage. Rate comparisons between regions are visual, and we realize that conclusions drawn from visual comparisons of limited earthquake catalogs must be limited in scope.

We seek to answer the following “chicken and egg” question: On the assumption that magma arriving from more than 20 km depth is represented by moment accumulation in the ms4.5 region, does it trigger a later response in the shallower ms2–3 (5–15 km depth) regions? To answer the question we look at magma-supply seismicity for systematic depth changes with time. Before 1959 it appears that the signal for deep magma supply precedes the signal for shallower magma supply by anywhere from about 1 to nearly 4 years; this inference is based on the interval between the deep *M*6.2 earthquake in April 1951 and the increases in shallower seismicity between 1952 and 1955 (fig. 8.11). Following the seismicity associated with the large subsidence during the 1960 euption, an increase in deep magma supply precedes an increase in shallower magma supply by nearly 6 years (approximately 1962 to 1967). During 1971–75, deep magma supply leads the seismicity

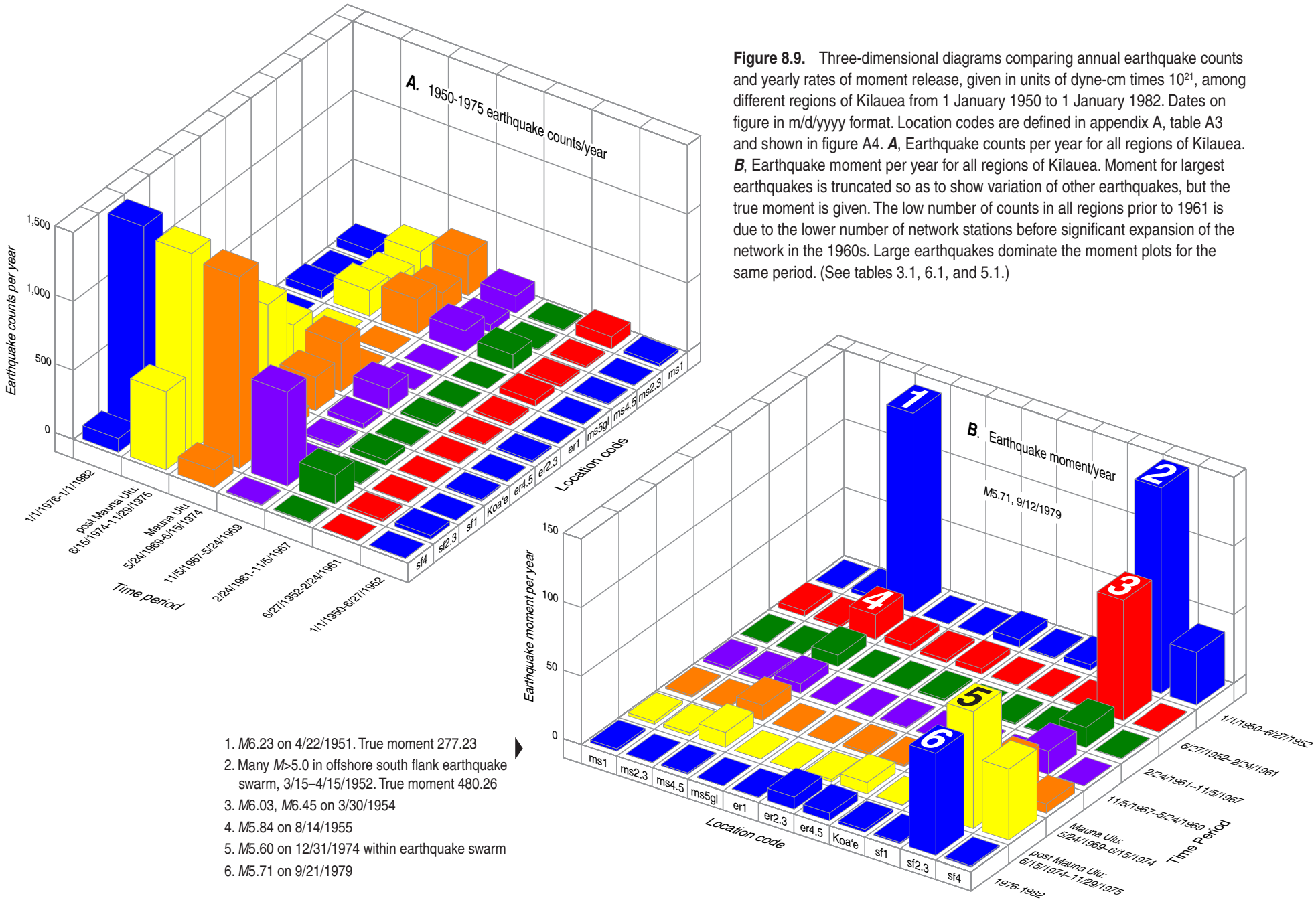

Figure 8.9. Three-dimensional diagrams comparing annual earthquake counts and yearly rates of moment release, given in units of dyne-cm times 10^{21}, among different regions of Kīlauea from 1 January 1950 to 1 January 1982. Dates on figure in m/d/yyyy format. Location codes are defined in appendix A, table A3 and shown in figure A4. ***A***, Earthquake counts per year for all regions of Kīlauea. ***B***, Earthquake moment per year for all regions of Kīlauea. Moment for largest earthquakes is truncated so as to show variation of other earthquakes, but the true moment is given. The low number of counts in all regions prior to 1961 is due to the lower number of network stations before significant expansion of the network in the 1960s. Large earthquakes dominate the moment plots for the same period. (See tables 3.1, 6.1, and 5.1.)

1. *M*6.23 on 4/22/1951. True moment 277.23
2. Many *M*>5.0 in offshore south flank earthquake swarm, 3/15–4/15/1952. True moment 480.26
3. *M*6.03, *M*6.45 on 3/30/1954
4. *M*5.84 on 8/14/1955
5. *M*5.60 on 12/31/1974 within earthquake swarm
6. *M*5.71 on 9/21/1979

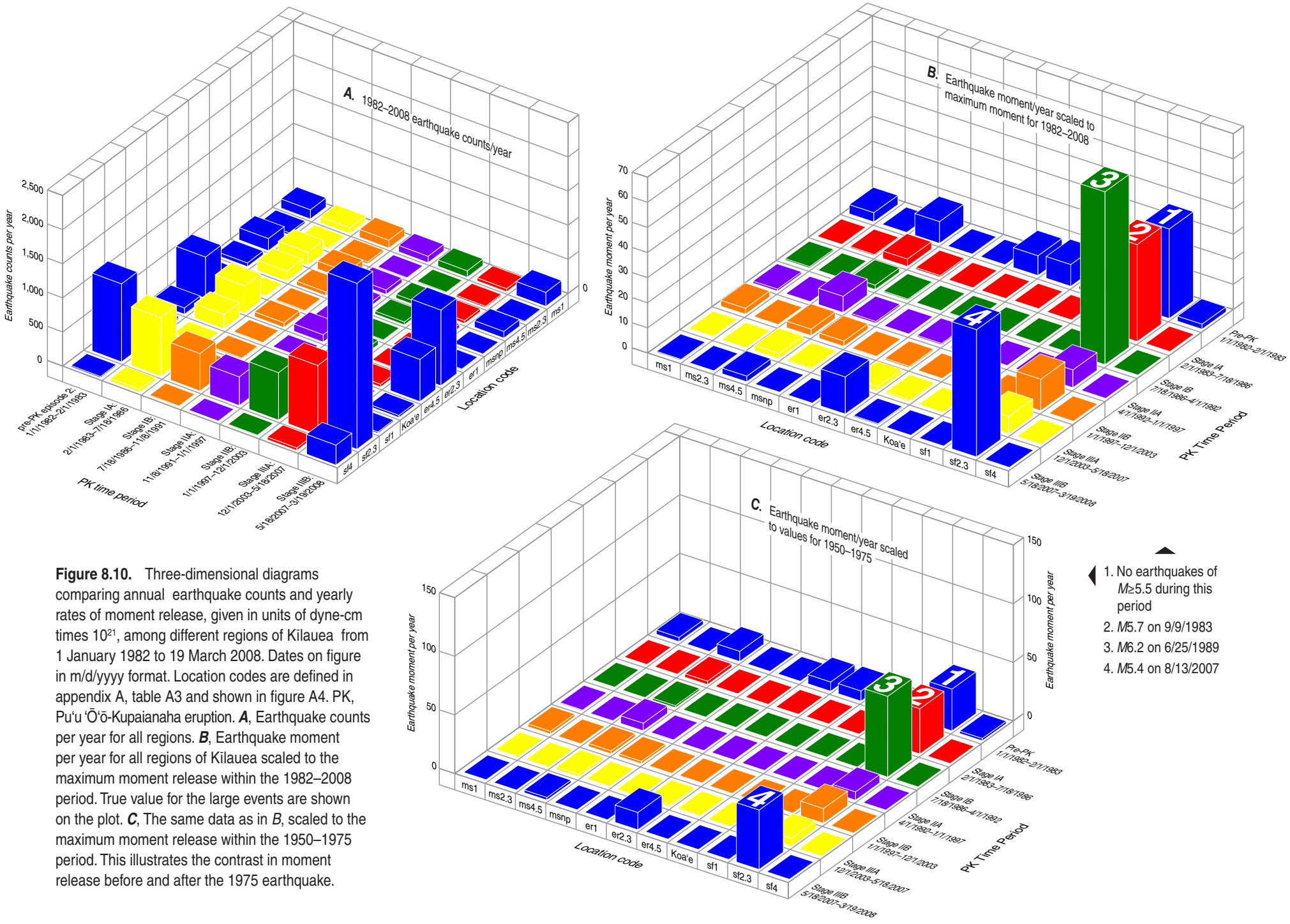

Figure 8.10. Three-dimensional diagrams comparing annual earthquake counts and yearly rates of moment release, given in units of dyne-cm times 10^{21}, among different regions of Kīlauea from 1 January 1982 to 19 March 2008. Dates on figure in m/d/yyyy format. Location codes are defined in appendix A, table A3 and shown in figure A4. PK, Pu'u 'Ō'ō-Kupaianaha eruption. ***A***, Earthquake counts per year for all regions. ***B***, Earthquake moment per year for all regions of Kīlauea scaled to the maximum moment release within the 1982–2008 period. True value for the large events are shown on the plot. ***C***, The same data as in *B*, scaled to the maximum moment release within the 1950–1975 period. This illustrates the contrast in moment release before and after the 1975 earthquake.

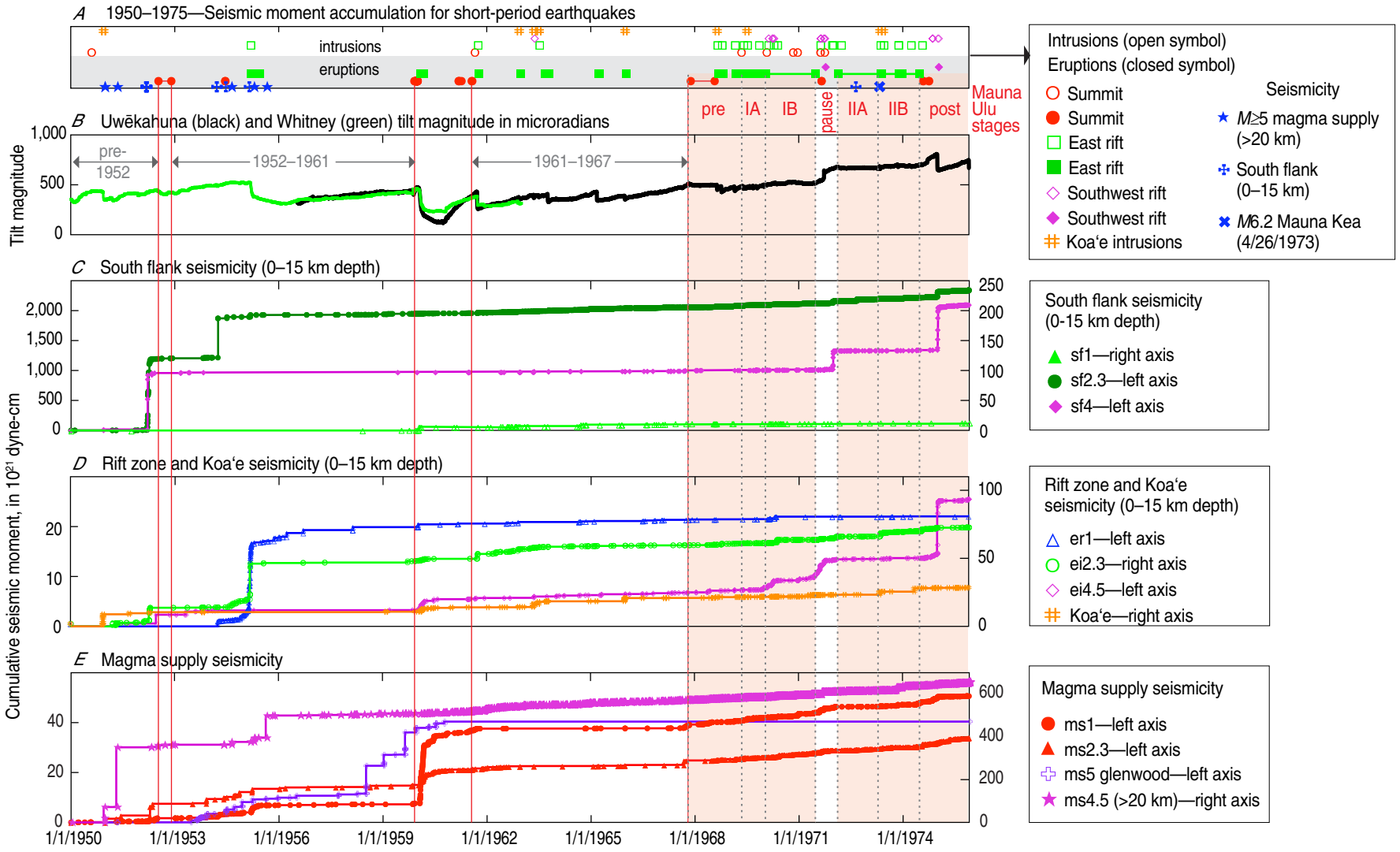

Figure 8.11. Graphs showing earthquake moment accumulation for short-period earthquakes in all regions of Kīlauea from 1 January 1950 to 29 November 1975 (up until the time of the *M*7.2 south flank earthquake). Dates on figure in m/d/yyyy format. Location codes are defined in appendix A, table A3 and shown in figure A4 (for example, er1 and sf2.3). From top to bottom, panel ***A*** shows times of eruption and intrusion; panel ***B*** shows the Uwēkahuna and Whitney tilt data; panels ***C***–***E*** show, respectively, seismicity beneath the south flank, rift zones and Koa'e, and the magma-supply regions. Vertical lines separate time intervals related to the summit eruptions of 1952, 1961 and 1967–68, as well as the stages of the Mauna Ulu eruption.

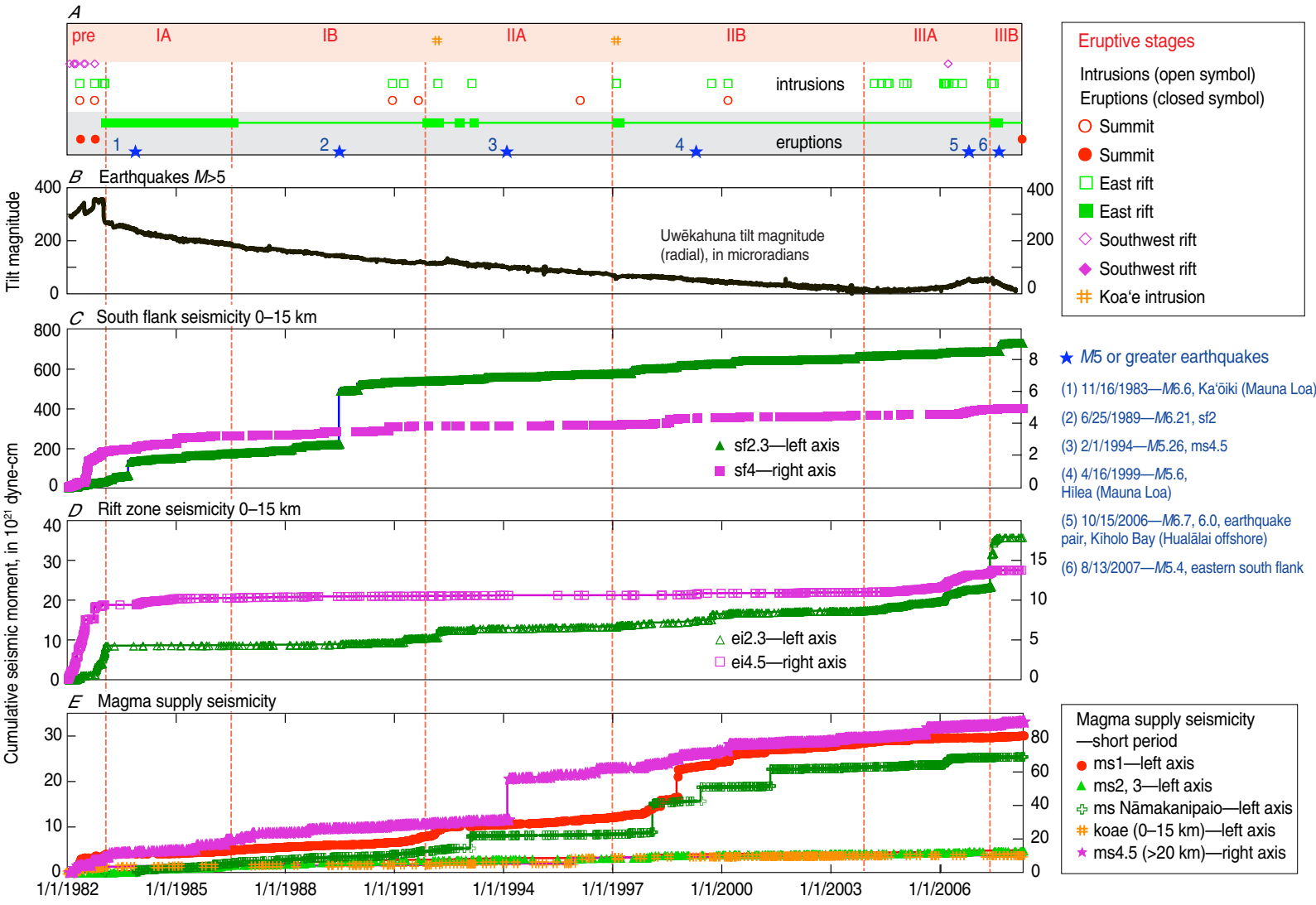

Figure 8.12. Graphs showing earthquake moment accumulation for short-period earthquakes in all regions of Kīlauea from 1 January 1982 to 1 April 2008 (including eruptive stages in the first 26 years of the Pu'u 'Ō'ō-Kupaianaha eruption). Dates on figure in m/d/yyyy format. Location codes are defined in appendix A, table A3 and shown in figure A4 (for example, ms1 and sf2.3). From top to bottom, panel ***A*** shows times of eruption and intrusion; panel ***B*** shows the Uwēkahuna tilt data; panels ***C–E*** show, respectively, seismicity beneath the south flank, rift zones and koae, and the magma-supply regions.

at 5–15 km by less than a month in late 1971 and by nearly a year between late 1973 and late 1974. The relations among deep and shallow long-period seismicity after 1972 (fig. 8.13) are unclear, perhaps because of a much smaller number of earthquakes.

Near Kīlauea's magma supply conduit, deep earthquakes tend to lead shallow earthquakes by years to months. During the eruption that began in 1983, the short-period earthquakes between 5 and 15 km depth (ms2 and ms3) were not active, so we make the comparison of changes in rate of the magma supply deeper than 20 km with magma supply shallower than 5 km (fig. 8.12). For the short-period earthquakes, the deeper magma supply again leads by up to 6 years (1985–1991) and 4 years (1994–1998), the lead time becoming less going forward in time, reaching only 3 months in late 2005-early 2006, and finally showing a nearly simultaneous increase at both depths from 1998 through early 2000. To the extent that the largest earthquake (and therfore the largest moment step) indicates magma supply, there is a 4-year lead of the deep February 1994 earthquake before the shallow September 1998 earthquake. The long-period seismicity shows the relation more clearly, the lead ranging from a difference of about 2 years in 1987–89 to 6 years between 1992 and 1998 (fig. 8.14).

The seismicity results suggest that deep magma supply drives the shallow response, initially with an apparent time delay measured in years. The shallowing of seismicity occurs in a general, diffuse sense, and there is no narrowly defined upward earthquake migration along a specific conduit. With continued use, the magma transport path from mantle to shallow storage becomes more open, resulting in a response within months of the shallow magma system to a change in rate of incoming magma from depth.

Magma Supply and South Flank Spreading—Who's the driver?

The spreading model for Kīlauea postulates a relation between deep magma supply and south flank spreading. Figures 8.15 (1950–75) and 8.16 (1983–2008) compare jumps in the cumulative moment in the deep magma supply (m) and the active central and eastern parts of the south flank (f). Jumps in the rate of moment release result from swarms or large earthquakes. Note that jumps from large-magnitude earthquakes are represented by red up-arrows, with the magnitude and true moment given on the plot.

The close time coincidence in jumps 2, 3, and 4 and the visual similarity of the two moment plots suggest an interpretable relation. In the 1950–75 period (fig. 8.15), the deep magma-supply jumps (m1–m5) lead (by 1.3–0.4 yr) or are very close behind (by 0.6–0.1 yr) the south flank jumps (f1–f5). By contrast, during the 1983–2008 Pu‘u ‘Ō‘ō-Kupaianaha eruption (fig. 8.16), the south flank jumps in earthquake moment (f1–f4) lead (by 5.4 to 0.4 yr, assuming the event associations made in the figures) the jumps in magma-supply earthquake moment (m1–m4). The implications of this shift are discussed below.

The relation of spreading rate to magma supply rate helps us to understand the mechanism of spreading and to answer the question of whether spreading is solely driven by magma supply. The reconstruction of spreading history shown above (figs. 8.6*A* and *C*) shows a low rate of south flank spreading during recovery from the 1924 collapse, and we postulate that the rate increases, beginning with the the pre-1952 inflation and continuing to the 1975 earthquake. There was a 3-m extension during the 1975 earthquake and a spreading rate between the earthquake and the beginning of the Pu‘u ‘Ō‘ō-Kupaianaha eruption that is slightly higher than rates preceding the earthquake (Delaney and others, 1998). During this period the magma supply rate also increased (fig. 8.5). Because the magma supply rate clearly increased following the recovery from the 1924 collapse, and on our assumption of low spreading rate before that time, we conclude that during the period from 1950 to 1983 magma supply drove spreading. This is consistent with the time delay separating deep magma-supply earthquake events from south flank seismicity (fig. 8.15) and also suggests that deep magma supply correlates with, and in 3 of the 5 cases, precedes flank spreading during this period.

During the Pu‘u ‘Ō‘ō-Kupaianaha eruption, motion of Kīlauea's south flank was mostly smooth and slightly declining, with small offsets for large earthquakes and eruptions. Spreading rates were lower at the beginning of eruption (fig. 8.6*A*), while the magma supply rate was higher (fig. 8.5) than in preceding periods. Throughout the eruption magma supply continued to increase, whereas the spreading rate remained constant or slightly declining within ±20 percent of the average rate (fig. 8.6*C*).

In order to explain the relation between magma supply and spreading rates across the beginning of eruption shown in figures 8.6 and 8.5 we propose that the 1975 earthquake reduced friction on the sliding surface (decollement) such that slumping and other gravity-driven forces became the dominant factor governing spreading rate rather than magma supply. Within the Pu‘u ‘Ō‘ō-Kupaianaha eruption, increases in magma supply were accommodated by dilating the rift zone and erupting magma with greater efficiency, rather than by accelerating the spreading rate. This is also consistent with the evidence that jumps in south flank moment release precede jumps in magma supply moment (fig. 8.16).

Figure 8.13. Graphs comparing seismic moment accumulation for short- and long-period magma supply earthquakes at Kīlauea for the period from 1 May 1972 to 1 December 1975. Long-period earthquakes were not tabulated before May 1972. Dates on figure in m/d/yyyy format. Location codes are defined in appendix A, table A3 and shown in figure A4 (for example, ms1). From top to bottom, panel ***A*** shows times of eruption and intrusion; panel ***B*** shows the Uwēkahuna tilt data; panels ***C*** and ***D*** show, respectively, short-period and long-period data. The long-period moments are only relative to each other and not absolute because a moment relation has not been defined.

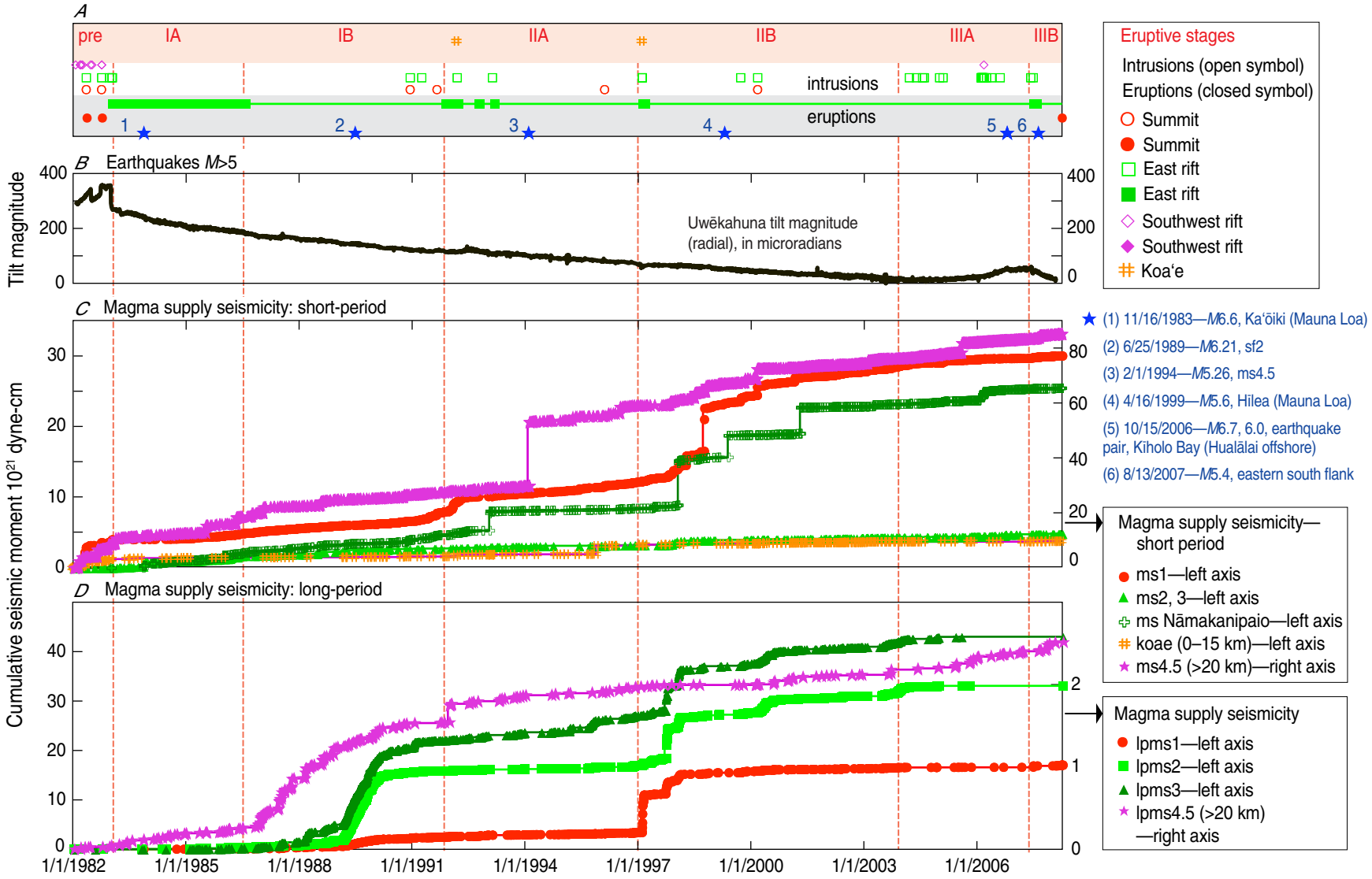

Figure 8.14. Graphs comparing seismic moment accumulation for short- and long-period magma supply earthquakes at Kīlauea for the period from 1 January 1982 to 1 April 2008 (including eruptive stages in the first 26 years of the Pu'u 'Ō'ō-Kupaianaha eruption). Dates on figure in m/d/yyyy format. Location codes are defined in appendix A, table A3 and shown in figure A4 (for example, ms1). From top to bottom, panel ***A*** shows times of eruption and intrusion; panel ***B*** shows the Uwēkahuna tilt data; panels ***C*** and ***D*** show, respectively, short-period and long-period data.

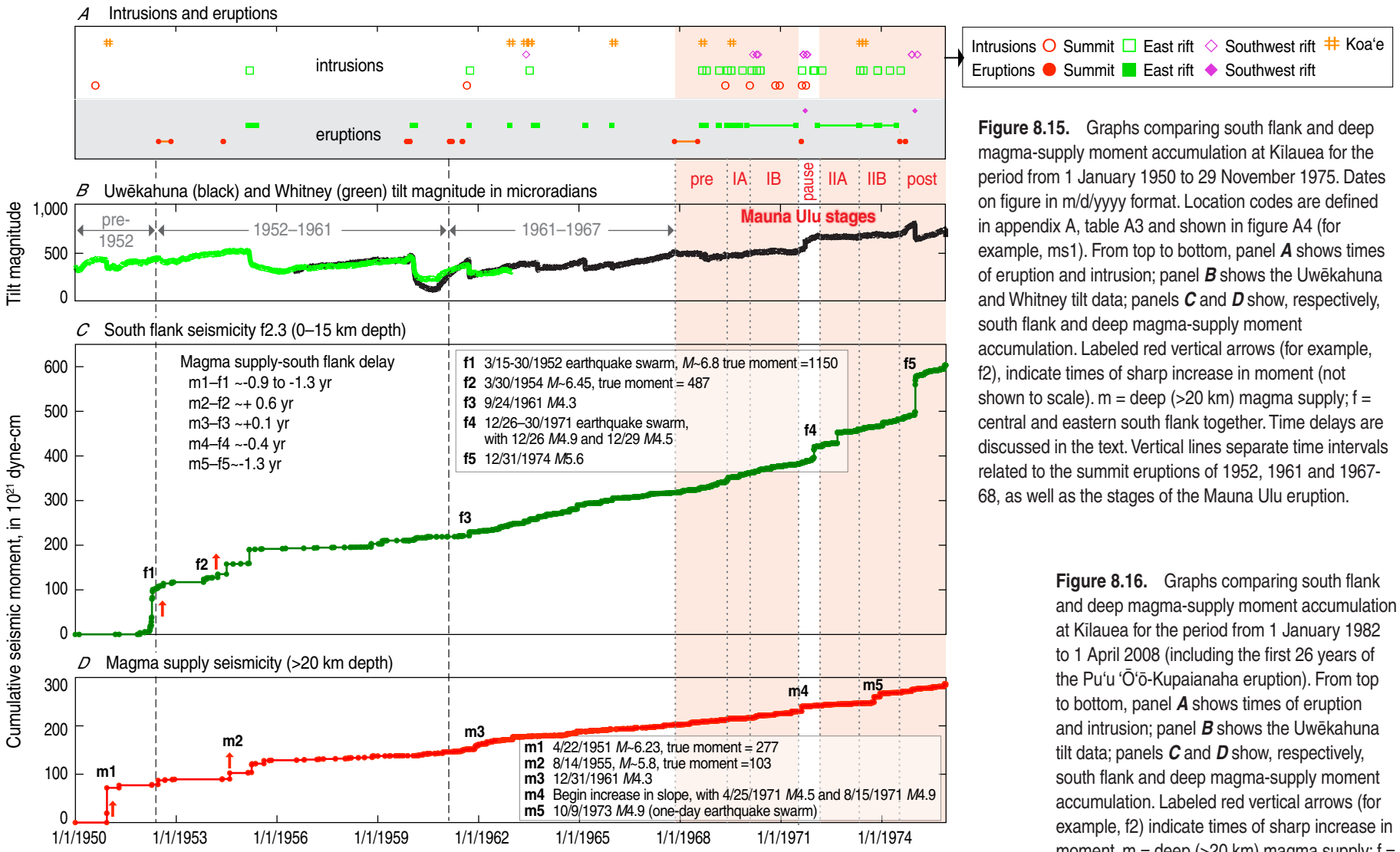

Figure 8.15. Graphs comparing south flank and deep magma-supply moment accumulation at Kīlauea for the period from 1 January 1950 to 29 November 1975. Dates on figure in m/d/yyyy format. Location codes are defined in appendix A, table A3 and shown in figure A4 (for example, ms1). From top to bottom, panel ***A*** shows times of eruption and intrusion; panel ***B*** shows the Uwēkahuna and Whitney tilt data; panels ***C*** and ***D*** show, respectively, south flank and deep magma-supply moment accumulation. Labeled red vertical arrows (for example, f2), indicate times of sharp increase in moment (not shown to scale). m = deep (>20 km) magma supply; f = central and eastern south flank together. Time delays are discussed in the text. Vertical lines separate time intervals related to the summit eruptions of 1952, 1961 and 1967-68, as well as the stages of the Mauna Ulu eruption.

Figure 8.16. Graphs comparing south flank and deep magma-supply moment accumulation at Kīlauea for the period from 1 January 1982 to 1 April 2008 (including the first 26 years of the Pu'u 'Ō'ō-Kupaianaha eruption). From top to bottom, panel ***A*** shows times of eruption and intrusion; panel ***B*** shows the Uwēkahuna tilt data; panels ***C*** and ***D*** show, respectively, south flank and deep magma-supply moment accumulation. Labeled red vertical arrows (for example, f2) indicate times of sharp increase in moment. m = deep (>20 km) magma supply; f = central and eastern south flank together. Time delays are discussed in the text.

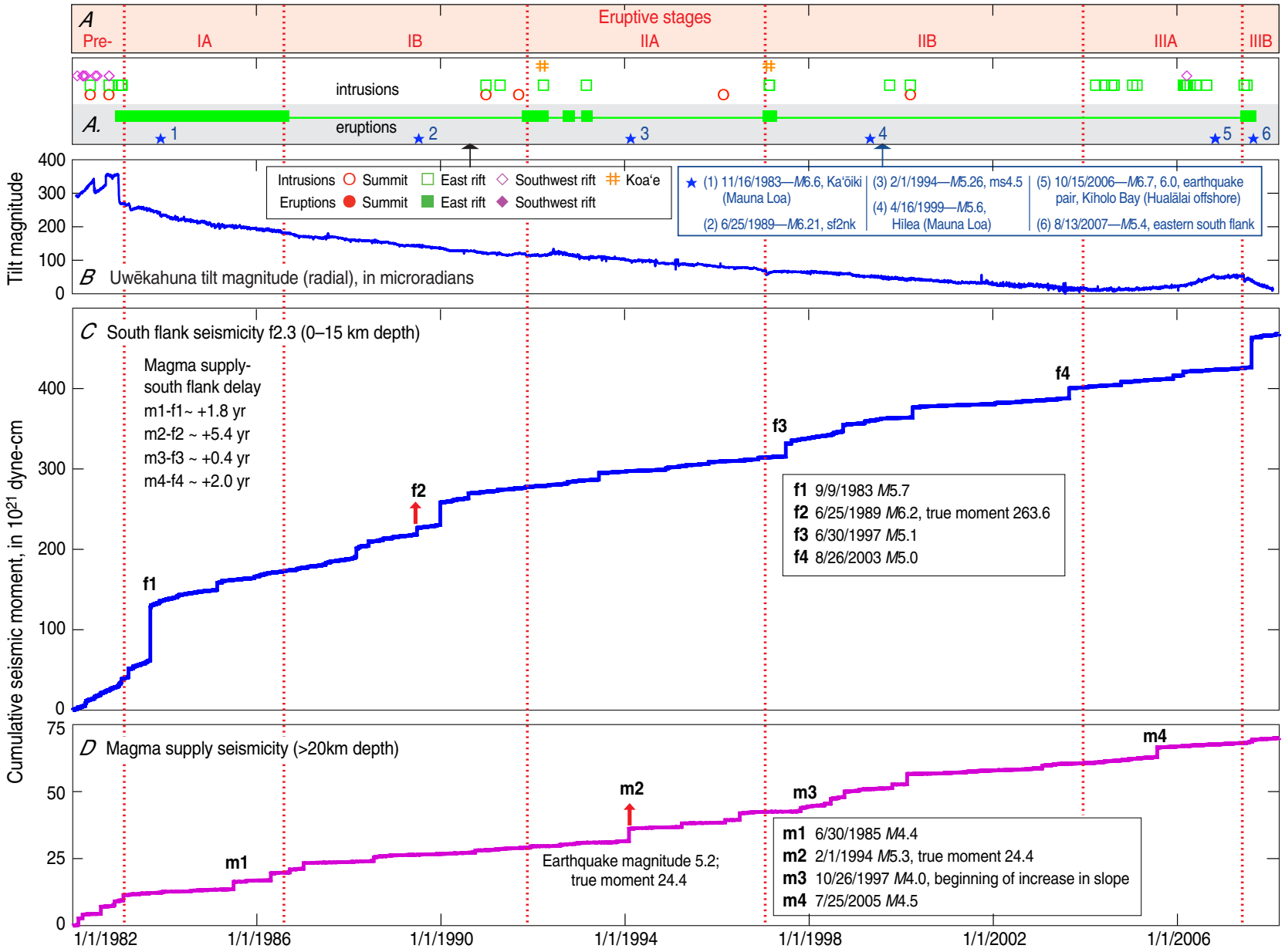
A
Pre-
IA
IB
Eruptive stages
IIA
IIB
IIIA
IIIB
intrusions
eruptions
A.
1
2
3
4
5
6
Intrusions Summit East rift Southwest rift Koa'e
Eruptions Summit East rift Southwest rift
(1) 11/16/1983—M6.6, Ka'ōiki (Mauna Loa)
(2) 6/25/1989—M6.21, sf2nk
(3) 2/1/1994—M5.26, ms4.5
(4) 4/16/1999—M5.6, Hilea (Mauna Loa)
(5) 10/15/2006—M6.7, 6.0, earthquake pair, Kīholo Bay (Hualālai offshore)
(6) 8/13/2007—M5.4, eastern south flank
Tilt magnitude
400
300
200
100
0
B Uwēkahuna tilt magnitude (radial), in microradians
C South flank seismicity f2.3 (0–15 km depth)
Magma supply-south flank delay
m1-f1~ +1.8 yr
m2-f2 ~ +5.4 yr
m3-f3 ~ +0.4 yr
m4-f4 ~ +2.0 yr
f1
f2
f3
f4
f1 9/9/1983 M5.7
f2 6/25/1989 M6.2, true moment 263.6
f3 6/30/1997 M5.1
f4 8/26/2003 M5.0
Cumulative seismic moment, in 10^21 dyne-cm
400
300
200
100
0
D Magma supply seismicity (>20km depth)
m1
m2
m3
m4
Earthquake magnitude 5.2; true moment 24.4
m1 6/30/1985 M4.4
m2 2/1/1994 M5.3, true moment 24.4
m3 10/26/1997 M4.0, beginning of increase in slope
m4 7/25/2005 M4.5
75
50
25
0
1/1/1982
1/1/1986
1/1/1990
1/1/1994
1/1/1998
1/1/2002
1/1/2006

Post-1983 History of Continuous Eruption

The Pu‘u ‘Ō‘ō-Kupaianaha eruption embodies many phenomena either not identified or not present during previous periods of activity. Here we discuss these phenomena, which were presented in chapter 7.

Pauses, Surges, Silent Earthquakes, and Suspected Deep Intrusions

Pauses, eruption surges (D-I-D events), suspected deep intrusions, and silent earthquakes all offer clues as to the state of the magma plumbing. Surges, first detected in 1996, can be interpreted to follow temporary blockage of the transport path between the summit reservoir depicted in figure 8.1 and the east rift vent (Cervelli and Miklius, 2003). The timing of inflation at Kīlauea's summit and the eruption site during surges suggests that magma was transmitted from the summit reservoir to the magma source beneath Pu‘u ‘Ō‘ō at rates of 0.54–1.58x10^6 m^3/day (Cervelli and Miklius, 2003, table 1), which translates to an average magma supply rate exceeding 0.20 km^3/year. This may be additional evidence in favor of a surge in magma supply associated with the 1997 eruption. After 2004, the surges lose their distinctive signature, perhaps because blockages were prevented by later increases in magma supply or by smoothing of irregular spots in the magma supply conduit.

In contrast to the surges, we consider that pauses, silent earthquakes, and suspected deep intrusions are all triggered by the deeper magma system beneath the rift zone that was first outlined by Delaney and others (1990). The precursory sequence shown in figure 7.7 of (1) long-period earthquake counts at 5–13 km depth below the summit, followed by (2) a small deflation without an eruption surge, suggests that the pauses were induced by temporary diversion of the deeper summit magma supply to feed intrusion beneath the east rift zone. Pauses lose their distinctive tilt and seismic signatures in 1991 during stage II of the eruption. The later pauses may be simply short interruptions due to temporary blockage of the shallow magma supply path with no precursory signs.

Suspected deep intrusions show a pattern of south flank seismicity similar to that of events documented in recent studies as "slow" or "silent" earthquakes (Cervelli and others, 2002b; Montgomery-Brown and others, 2009; Segall and others, 2006). All suspected deep intrusions are revealed by earthquake swarms beneath the south flank without a main shock, and some are accompanied by a few shallow rift earthquakes. Suspected deep intrusions within the period in which silent earthquakes have been identified are listed in table 8.2. The larger events identifed as silent earthquakes with an earthquake swarm would also be classified by us as suspected deep intrusions. Some of the events with smaller south flank displacements are accompanied by very few earthquakes, insufficient to specify a suspected deep intrusion by seismicity alone. Significantly, there are a few events since the start of continuous geodetic monitoring in 1998 with an earthquake pattern resembling that of a suspected deep intrusion that have not been identified as being associated with a spreading step.

The patterns of south flank earthquakes shown by suspected deep intrusions are shown in figure 8.17. South flank seismicity characteristic of suspected deep intrusions began as early as 1962. The "Kalapana Trail" south flank events mentioned in chapter 4 (fig. 4.12) are possible candidates for suspected deep intrusions because they occur in closely spaced sequences beneath the south flank and are isolated in time from other seismicity. However, because the locations of such small-magnitude events are so uncertain within the seismic network available at that time, we hesitate to label them as such and consider the possibility that they could even represent mislocated rift events. The earliest events that have the pattern of suspected deep intrusions occur in 1965 (figure 8.17*C*).

Suspected deep intrusions likely occur when pressure is applied to the deep magma system beneath the rift zones. The earliest examples may have been triggered following the swarms of magma-supply earthquakes at 30-km depth beneath Kīlauea Caldera that began in 1961 and died out by the end of 1965. These deep swarms are interpreted to accompany increased magma supply and also could trigger suspected deep intrusions. Over the 50 years between 1961 and 2011, we infer that suspected deep intrusions accompanied by a swarm of south flank earthquakes were probably associated with a spreading step. It is possible that a combination of a previous intrusion and the occurrence of suspected deep intrusions may provide a rationale for the absence of seismicity during some east rift eruptions. For example, the intrusion of February 1993 (table 7.3) extended downrift to the site of the January 1997 eruption and intrusion (table 7.4). The force of the 1993 intrusion near the future eruption site, combined with suspected deep intrusions at site SDI 2 on 11–12 September 1993 and 25–26 October 1994 (table 7.3; fig. 7.8) may have dilated the rift zone sufficiently to explain the absence of rift seismicity preceding the January 1997 event.

Relations Between Kīlauea and Mauna Loa

In chapter 1 we noted that the growth of Kīlauea's and Mauna Loa's rift zones has been unequal and complementary—that is, Mauna Loa's long southwest rift zone is paired with Kīlauea's stunted southwest rift zone, and Kīlauea's long east rift zone is paired with Mauna

Table 8.2. Silent earthquakes and suspected deep intrusions[1].

[Rows highlighted in **bold type** represent events identified by us as "suspected deep intrusions" and in the published literature as "silent earthquakes"; dates in m/d/yyyy format. Events identified by us as suspected deep intrusions, but not published as geodetically identified silent earthquakes, are listed in event tables in individual chapters]

Date	P[2]	D [3] (cm)	Loc.[4]	SDI?[5]	No.[6]	Comment	Figure[7]
2/20/1998	0.89	0.12		no	2	Not identified as suspected deep intrusion	-
9/19/1998	**1.0**	**0.72**	**SDI 2**	**yes**	**12**	**South flank 9/19–20/1998**	**G29**
1/10/1999	0.55	0.21			2	Not identified as suspected deep intrusion	-
4/27/1999	0.7	-			0	Not identified as suspected deep intrusion	-
11/21/1999	0.85	0.41			0	Not identified as suspected deep intrusion	-
5/29/2000	**0.75**	**0.17**	**SDI 2**	**yes**	**25**	**South flank 5/29–30/2000**	**7.11**
11/9/2000	1.0	1.43	SDI 2	yes	11	South flank 11/8–9/2000	G36
9/19/2001	0.55	0.06				Not identified as suspected deep intrusion	G39
8/21-22/2002			SDI 2	yes	9	Not identified as a silent earthquake[8]	G44
8/28-29/2002			SDI 2	yes	8	Not identified as a silent earthquake	G44
12/17/2002	0.96	0.12		yes	5	Not identified as suspected deep intrusion	G45
7/3/2003	**0.99**	**0.62**	**SDI 3**	**yes**	**10**	**South flank 7/1–2/2003**	**G48**
12/22/2003			SDI 2	yes	7	Not identified as a silent earthquake	G51
5/6/2004	0.7			no	2	Not identified as suspected deep intrusion	-
1/26/2005	**1.0**	**2.06**	**SDI 2**	**yes**	**55**	**South flank 1/25–27/2005**	**G60**
6/27/2005	0.56	0.22		no		5 south flank earthquakes 6/26–28	-
3/16/2006			SDI 2	yes	13	Not identified as a silent earthquake	G70
4/16/2007	0.55	0.07		no	2	Not identified as suspected deep intrusion	
6/18/2007		4.01	SDI 2	yes			7.13; G79

[1]Events shown in this paper and in table 1 of Montgomery-Brown and others (2009).

[2]Probability of event being a silent earthquake (Montgomery-Brown and others, 2009, table 1, column 7).

[3]Displacements calculated from north and east components of GPS displacements for south flank GPS sation KAEP (Emily Montgomery-Brown, written commun,. 2011).

[4]Referenced to chapter 5, figure 5.2.

[5]yes = south flank swarm corresponds to SDI patterns of chapter 5, figure 5.2.

[6]Number of south flank earthquakes.

[7]Figure references are to chapter 7. Text figures are designated 7.x; appendix G figures are designated Gxx.

[8]Aftershock sequenec following a pair of *M*3.6, 3.0 earthquakes?

Loa's short northeast rift zone. Mauna Loa being older, this implies that its early growth favored the southwest rift zone. Later, the vigor of Mauna Loa's southwest rift development prevented Kīlauea from growing in that direction. Instead Kīlauea was forced to grow to the east, with the result that Mauna Loa's later development was blocked in that direction.

There is a long-term relation between Kīlauea and Mauna Loa eruptive activity, Kīlauea being most active when Mauna Loa is quiet and vice versa (Klein, 1982). Figure 8.18 compares the inferred magma filling rates for Kīlauea with the timing and volume of Mauna Loa eruptions. Eruption volume is the best practical measure of Mauna Loa productivity, whereas long-lived caldera filling and frequent or long-lasting eruptions make cumulative volume the best measure for Kīlauea. The increase in Kīlauea's eruption frequency and magma supply rate, and simultaneous decrease in Mauna Loa's eruption frequency, after 1950 is clearly visible. Unfortunately, the Mauna Loa record only begins in 1843, and little is known of the record before that time. A brief 1832 summit eruption is mentioned in the literature (see, for example, Goodrich, 1833), but its products have been covered by younger lavas. Modern mapping has identified only one eruption whose age could fall between 1790 and 1843 (Frank Trusdell, oral commun., 2011). The absence of significant Mauna Loa volcanism that can be confidently dated between 1790 and 1843 may be one factor controlling the very high filling rates at Kīlauea during the early part of the 19th century, and the reduced activity of Kīlauea after 1840 may correlate with the onset of more frequent activity at Mauna Loa (chap. 2). Thus there are two definite changeover times—from Kīlauea to Mauna Loa in 1840 and back again in 1950[30].

[30] Research by Frank Trusdell and Don Swanson has documented this relationship back in time (see, for example, Trusdell, 2012).

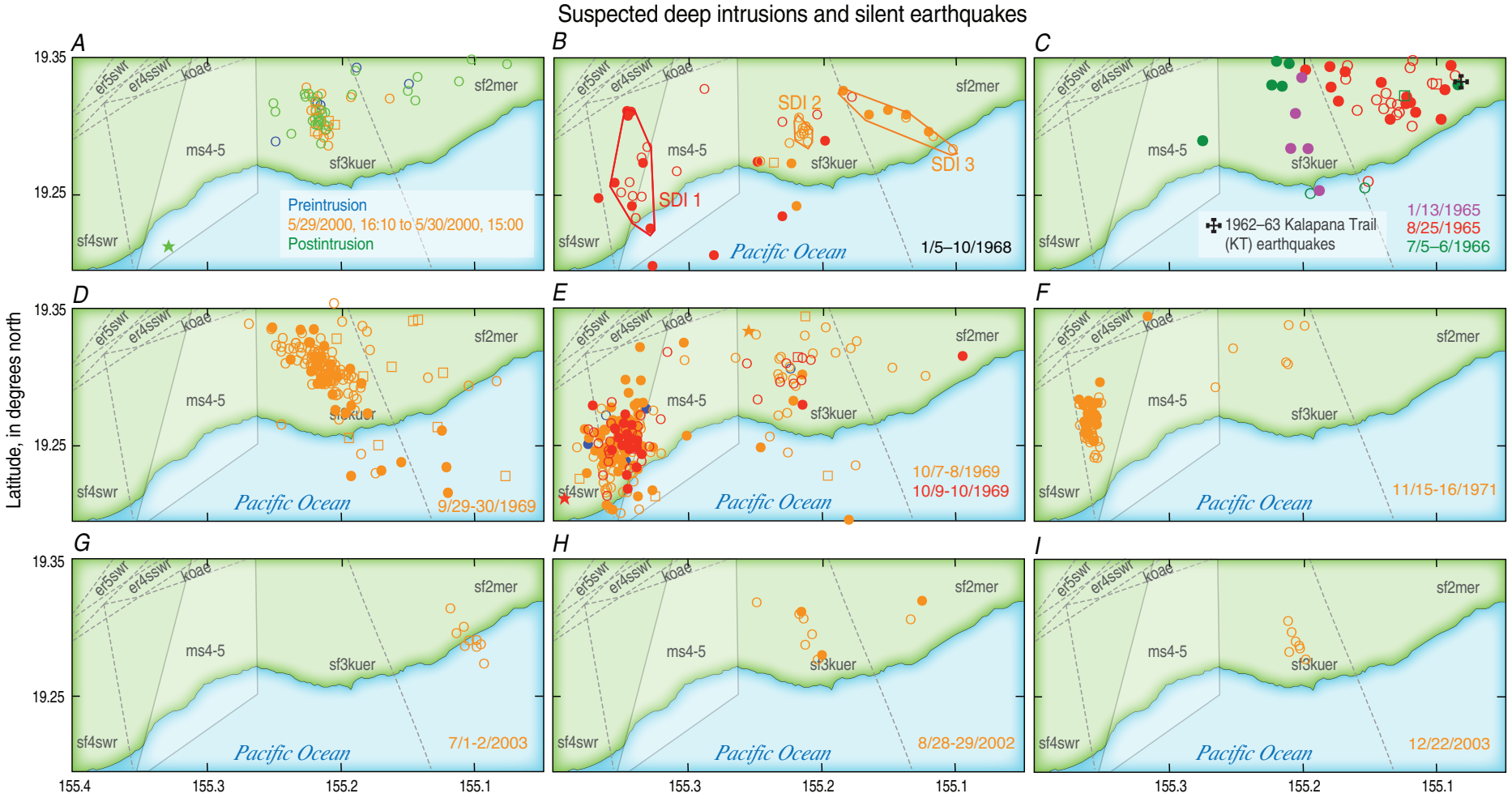

Note: documented silent earthquake in panel *A* on 5/29/2000 (Montgomery-Brown and others., 2009, table 1); suspected deep intrusion zone active for several more days as a broken swarm.

Figure 8.17. Maps showing seismicity of silent earthquakes (Montgomery-Brown and others, 2009) and suspected deep intrusions (this report, keyed to figure numbers) at Kīlauea. Dates on figure in m/d/yyyy format. Symbols for depth ranges apply to all figures. ***A***, 29–30 May 2000 (see fig. 7.11). Identified as both a silent earthquake and a suspected deep intrusion. ***B***, 5–10 January 1968 (see fig. 5.2). Suspected deep intrusions are found in three locations labeled, from west to east, SDI 1, SDI 2 and SDI 3. ***C***, 13 January 1965, 25 August 1965, and 5–6 July 1966 (see fig. 4.12). These are the earliest indications of the earthquake pattern associated with suspected deep intrusions. These are located near sites SDI 2 and 3 (see part B for site locations). ***D***, 29–30 September 1969 (see appendix E, fig. E17). An exceptionally strong earthquake swarm beneath site SDI 2. ***E***, 7–10 October 1969. A closely spaced (in time) pair of exceptionally strong earthquake swarms beneath sites SDI 1 and 2 . ***F***, 15–16 November 1971 (see appendix E, fig. E51). An exceptionally strong earthquake swarm beneath site SDI 1. ***G***, 1–2 July 2003 (see appendix G, fig. G48). A suspected deep intrusion that precedes by one day an identified silent earthquake (see table 8.2). ***H***, 28–29 August 2002 (see appendix G, fig. G44). A suspected deep intrusion not identified as a silent earthquake (see table 8.2). ***I***, 22 December 2003 (see appendix G, fig. G51). A suspected deep intrusion not identified as a silent earthquake (see table 8.2).

It is known that Mauna Loa and Kīlauea lavas can be distinguished chemically (see, for example, Wright, 1971), suggesting their derivation from separate mantle sources. Yet over historical time their eruptive activity has favored one volcano over the other, thus suggesting some sort of connection related to magma supply. The relative eruption frequency and chemical differences have been reconciled by postulating partial melting in different parts of the Hawaiian mantle source volume (Wright and Klein, 2006).

There have been instances in historical time during which both volcanoes were in eruption. The continuous activity at Kīlauea between 1907 and 1924 appears to have had no affect on Mauna Loa's eruptive cycles dating from 1843. The Mauna Loa eruption of 1984 occurred during episode 18 of the Kīlauea eruption that began in 1983, with no change in seismicity or ground deformation to indicate that either volcano had influenced the other at a shallow level. Another case in point is the return to activity of Kīlauea in 1952 following Mauna Loa's largest historical eruption in 1950. High seismicity associated with Mauna Loa continued for nearly ten years following the eruption, belying the fact that its activity would be greatly curtailed between then and now (2010) as Kīlauea entered a period of increasing magma supply.

It is by no means obvious what triggers a switch that favors eruption of one volcano over the other, but we suspect that mantle stresses are involved. We have looked for and not found any seismic indication prior to Kīlauea's reinflation in 1950 to indicate that a major switch of eruptive activity would occur, and the cause of a switch from one volcano to the other remains an area for further research (compare Gonnermann and others, 2011).

Evolution of Kīlauea's Plumbing Between 1823 and 2008

As a context for interpreting Kīlauea's behavior after the arrival of European missionaries in 1823, we go back in time to the formation of the ʻAilāʻau shield (whose surface is seen north and east of the present caldera) (Clague and others, 1999) and the present caldera (Clague and others, 1999; Swanson, 2003, 2009; Swanson and others, 2012). The ʻAilāʻau summit shield-building took place over about 50 years, ending at about 1470 C.E.[31]. During that time we presume that Kīlauea's rift zones were unable to accept magma and the south flank was locked, implying the temporary absence of seaward spreading. Soon after, Kīlauea's summit collapsed to an unknown depth to form a caldera during dates estimated at 1470–1510 C.E. A period of explosive eruption ensued, ending in 1790 C.E. with a climactic eruption that killed Hawaiian people marching across Kīlauea's summit (Dibble, 1843; Swanson and Christiansen, 1973; Swanson and Rausch, 2008). A 1790 eruption on Kīlauea's lower east rift zone has been identified by modern mapping (Trusdell and Moore, 2006), indicating that the east rift zone reopened sometime during the period of explosive eruption. This may also have been a time when the deep magma system below the east rift zone and above the decollement was rejuvenated.

When the missionaries arrived in 1823, the floor of Kīlauea Caldera contained an active lava lake over nearly its entire area (Ellis, 1825), which we interpret as recovery from a massive magma draining that probably occurred at the time of the culminating explosive activity of 1790. In successive disappearances of magma from

[31] The Common Era (C.E.) begins with year 1 of the Gregorian calendar.

the caldera during the 19th century we surmise that the entire magma system, encompassing sources 1 and 2, and possibly 3 as shown in chapter 2 (fig. 2.4), was drained and refilled. Earthquake swarms during the 19th century indicate that both the southwest and east rift zones were open to accept intrusions. The diminished rate of earthquake activity after 1840 is ascribed to both recovery from the 1790 draining and the onset of heightened eruptive activity at Mauna Loa. The century ended with Halema‘uma‘u as a single vent, only sporadically active at its bottom.

Kīlauea has alternated between higher and lower magma activity on a time scale of decades. Two distinct periods of magmatic activity before 1894 and after 1950 are separated by the summit collapse of 1924. Magma gradually returned to Halema‘uma‘u beginning in 1907, leading to a new lava lake and periodic overflow onto the caldera floor beginning in 1918. The lava lake and overflows were both fed from the shallow source 1. Source 2 was first distinctly evident to modern observation in the collapse of 1922. A broad regional uplift in 1918–19 was matched by an equally large regional subsidence accompanying the summit collapse in 1924. The Halema‘uma‘u collapse and phreatic eruption of May 1924 ended the lava lake activity, and the last draining of sources 1–3 in 1924 ended with a large intrusion into the lower east rift zone. The events of 1924 stabilized the relation between the rift zones and south flank, such that for several decades up to March 1950, the caldera remained at the post-1924 collapse level and the dominant magma movement was recovery of deep source 3. During the period 1924–50, small eruptions in Halema‘uma‘u used up the remnants of source 1, and source 2 may have been involved in intrusions of 1937 and 1938. Recovery was complete in March 1950, when inflation began in response to pressure generated within source 2. During the entire period of recovery the south flank remained locked and intrusions occurred with minimal seaward spreading.

Events preceding the 1952 eruption in Halema‘uma‘u are critical to Kīlauea’s subsequent history and demonstrate how changes at different parts of Kīlauea trigger each other. The deep earthquake swarm of December 1950, followed by the single deep earthquake of April 1951, coincided with and perhaps initiated a higher magma supply rate. The higher magma supply also served to trigger the intense offshore south flank swarm of March-April 1952, which we believe led to the unlocking of the south flank[32]. The increase in magma supply rate at Kīlauea is also a consequence of the great decrease in the rate of Mauna Loa activity following its large eruption in June of 1950. By 1952 one can definitely identify the traditional summit reservoir (source 2) as a source for resupply of the lower east rift eruptions of 1955 and 1960, as well as a source for middle and upper east rift eruptions from 1961 onward. Suspected deep intrusions (SDI) occur from at least 1961, at least some of which may have been associated with south flank spreading steps. If SDIs occurred before 1961, they would not have been detectable by the primitive seismic network, so it is unknown when they began. Magma supply and spreading rates increased following the 1967–68 summit eruption and continued to increase throughout the 1969–74 Mauna Ulu eruption.

The inability of Kīlauea during the 1960s to cope with increasing magma supply through release by eruption led to increased intrusive and eruptive activity on the southwest side of the volcano, which in turn led to the 1975 *M*7.2 south flank earthquake. Recovery from the effects of the earthquake occurred over the next 8 years, with episode 1 of the Pu‘u ‘Ō‘ō-Kupaianaha eruption in 1983 being the final event of the 1975 recovery. The consequences of the 1975 earthquake and the associated large component of both seaward spreading and rift dilation led to (1) a rift readily able to initally accept magma through numerous intrusions, (2) the development of an east rift zone plumbing that was able to sustain a decades-long east rift eruption accompanied by continuous deflation of Kīlauea’s summit, and (3) the freeing of the south flank to move by gravity alone, evidenced by the decoupling of spreading rate from magma supply rate during the long and still ongoing east rift eruption that began in 1983.

A final crisis in the pre-2010 history ensued following the return to inflation of Kīlauea’s summit in 2004 coupled with a great increase in magma supply represented by a large temporary increased output of CO_2 at Kīlauea’s summit from mid-2004 to mid-2005. Incomplete accommodation of the still-high magma supply rate in the Pu‘u ‘Ō‘ō-Kupaianaha eruption resulted first in a new small eruption and large east rift intrusion in June 2007, followed a month later by new vents on the east rift. As in the time preceding the 1975 earthquake, these events from additional magma supply were accompanied by summit inflation and increased seismicity in the southwest sector of the volcano. A second area of eruptive activity began in March 2008 as a lava pond visible below the surface of Halema‘uma‘u. The open vent in Halema‘uma‘u

[32] The many south flank earthquakes documented in the 19th century (Klein and Wright, 2000) are interpreted to involve stress release without seaward spreading on the decollement, and they probably were triggered by a massive stress redistribution caused by the great 1868 Ka‘ū earthquake (Klein and others, 2006). Stress release without a spreading step also occurred during the south flank earthquake of 25 June 1989 (fig. 8.6*C*). During the 1989 earthquake stress relief was interpreted to occur on shallower subhorizontal planes (Arnadottir and others, 1991), with perhaps an additional vertical component (Bryan, 1992). We favor a similar interpretation for the events occurring before March 1950.

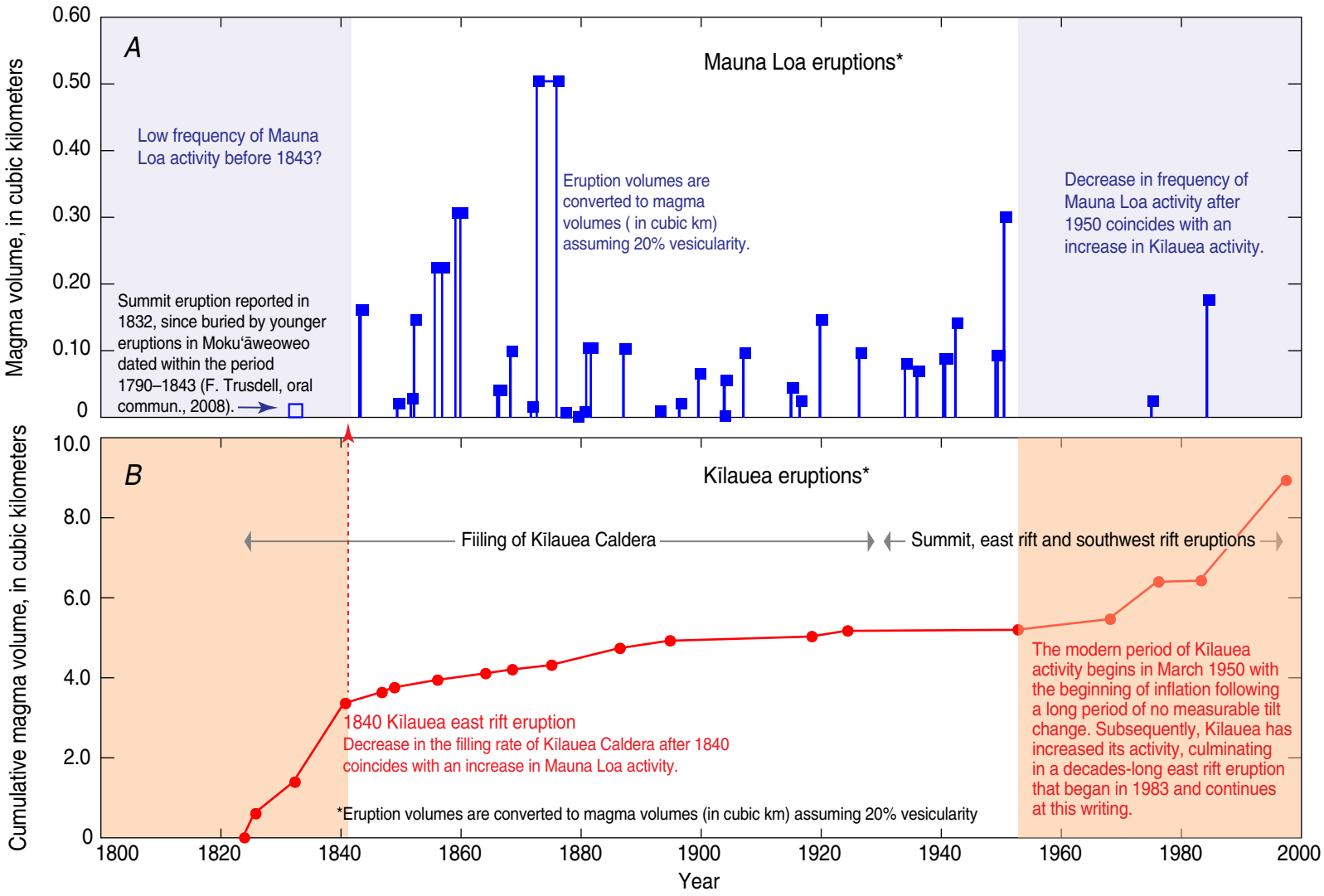

Figure 8.18. Graphs showing rates of filling of Kīlauea Caldera and volumes of later eruptions compared to frequency and volume of Mauna Loa eruptions. Times and volumes of Mauna Loa eruptions (***A***) are compared with filling rates at Kīlauea (***B***). Periods of high Mauna Loa activity correspond to periods of lower Kīlauea activity, as shown by slope of curve of cumulative magma volume, in agreement with previous work (for example, Klein, 1982).

has continued its activity to the present with no waning of the east rift eruption, marking the first time in Kīlauea's recorded history that summit and rift have been simultaneously active.

The combined data for the period 1950–2008 demonstrate a remarkably integrated magmatic system in which the response to the pressure of an increasing magma supply from depth occurs in the following ways: (1) the mantle supplies more magma and the volcano's behavior responds, or (2) the volcano dilates or spreads and encourages the mantle to send more magma, or (3) both happen together because the system is finely balanced. The attempt to erupt magma at Kīlauea's summit is fraught with difficulties related to the unique properties of magma and the interaction of magma with the complex structure of the volcanic edifice. Any resistance to upward movement of magma results in pressure being applied laterally. As long as the rifts are able to accept magma, magma will stay at a lower elevation, and stress is preferentially relieved by rift eruption and intrusion, and by movement of the south flank. In general, after stress is applied during larger rift intrusions, the south flank responds with increased seismicity. However, the response can be reversed when the flank earthquake is very large, as shown by the increased number of rift intrusions in the years following the large south flank earthquake of November 1975.

Eruptions in Halema'uma'u that last longer than a few days offer a different form of stress relief, eventually manifested by the lessening of seismic activity in all parts of the volcano. Yet this stress relief is temporary. The answer to the question posed by one of us many years ago as to why summit eruptions end (Wright and Fiske, 1971, p. 52) can now be viewed as a problem in partitioning of magma between the summit reservoir and the fluid core of the rift zone (compare Wright and Klein, 2008). As long as the rift is available, sustained summit activity is not possible and summit eruptions will end when it becomes easier for magma to move laterally than to move up. The long-term continuity of rift eruptions depends on the development of a stable conduit connecting the fluid core of the rift zone to the surface, such that pressure remains constant and the magma flow is sufficient to resist cooling against the walls. In general, the conduit system is not perfectly open. Cooling and the associated increase of magma viscosity acts to close conduits, causing a back-pressure that results in reinflation of Kīlauea's summit. The ongoing east rift eruption that began in 1983 has built an edifice in much the same way as earlier eruptions such as the one that formed the Heiheiahulu shield and lava field, but the east rift edifice built during this eruption is not high enough to stop the eruption. The most likely circumstance that would end this eruption is a change applied to the mantle source region such as to favor renewed and more frequent activity on Mauna Loa than is seen at present.

During Kīlauea's many cycles of breakdown and recovery, different parts of the plumbing may be more or less active, and the parameters of magma storage and transport may change. These changes are principally because of increased magma activity or the increased occurrence of large, deep, conduit earthquakes. The crisis and recovery cycles offer a sobering reminder for eruption and earthquake prediction, and for hazard evaluation. Crisis and recovery can each be anticipated by looking at both deformation and seismic patterns, but the nature of both crisis and recovery may vary greatly from one instance to the next. Our view is that the volcano's behavior is governed by nonlinear dynamics in which several systems interact. Each crisis changes the ground state of the Kīlauea edifice such that all seismic, deformation, and magma parameters used in monitoring are set to a new and unknown baseline. Continuous monitoring must determine the baselines and departures from it, but changes in the volcano state render long-term eruption and earthquake prediction inherently uncertain.

Supplementary Material

Supplementary material for this chapter appears in appendix H, which is only available in the digital versions of this work—in the DVD that accompanies the printed volume and as a separate file accompanying this volume on the Web at http://pubs.usgs.gov/pp/1806/. Appendix H comprises the following:

Tables H1–H3 contain accumulated earthquake counts and moment for all regions plotted in figures 8.11 and 8.12.

Table H4a gives volumes of the three magma batches erupted at Halema'uma'u in 1952, 1961, and 1967–68 that are identified in eruptions between 1952 and the beginning of the Mauna Ulu eruption in May 1969.

Table H4b gives additional volumes inferred for intrusions over the same period of time. See text for interpretations using these quantities.

Figure H1 shows the location of edm and GPS stations used in constructing figures 8.6 and 8.7.